TRANSPORT PHENOMENA IN A CLOUD OF SOLID PARTICLES, DROPS OR BUBBLES

A Thesis Submitted
in Partial Fulfilment of the Requirements
for the Degree of
MASTER OF TECHNOLOGY

By

SATISH KUMAR

to the
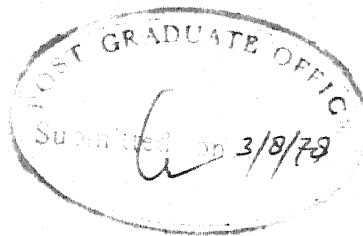**DEPARTMENT OF CHEMICAL ENGINEERING**
INDIAN INSTITUTE OF TECHNOLOGY, KANPUR
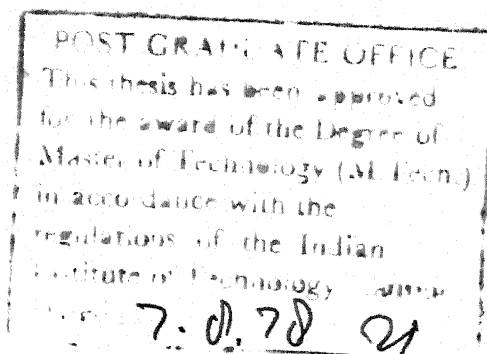AUGUST, 1978

LOVINGLY DEDICATED

TO

N A V E E N

CERTIFICATE

This is to certify that the thesis entitled 'TRANSPORT PHENOMENA IN A CLOUD OF SOLID PARTICLES, DROPS OR BUBBLES' by SATISH KUMAR is record of work carried out under my supervision and has not been submitted elsewhere for a degree.

August 2, 1978

S.K. Gupta, Ph.D.
Assistant Professor
Department of Chemical Engineering
Indian Institute of Technology,
Kanpur-208016

ACKNOWLEDGEMENTS

LIST OF TABLES

LIST OF FIGURES

SYNOPSIS

of the

DISSERTATION ON

TRANSPORT PHENOMENA IN A CLOUD OF SOLID PARTICLES,
DROPS OR BUBBLES

Submitted in Partial Fulfilment of
the requirements for the degree of

MASTER OF TECHNOLOGY

in

CHEMICAL ENGINEERING

by

SATISH KUMAR

Department of Chemical Engineering
Indian Institute of Technology
KANPUR

The complications in transport phenomena of dispersed
or particulate systems due to non-spherical particle sizes and
a distribution in drop or particles sizes have been pointed
out. A cell model has been used to obtain the creeping flow
velocity profile around and drag on an oblate (or prolate)
spheroidal particle located in a cloud of identical oblate
(or prolate) spheroidal particles all of which are oriented
with their minor (or major)axes in the mean flow direction.
The predicted settling velocities agree satisfactorily with
experimental data for spheres when the spheroidal particle
eccentricity tends to unity corresponding to a sphere. The
mass transport rate to a single active oblate (or prolate)
·spheroidal particle surrounded by a cloud of inactive identical

oblate (or prolate) spheroidal particles through which a fluid is having creeping motion has also been obtained for large Schmidt numbers. Predicted Sherwood numbers agree quite well with the experimental values of Sherwood numbers for an active sphere in a cloud of inactive spheres. Using Sirkar's [17] velocity field in creeping flow around a test drop (or bubble) placed in a random size-distributed cloud of drops (or bubbles), a solution of the convective diffusion equation is also obtained for high Schmidt numbers. The expected value of the quantity $Sh\ Pe^{-1/2}$ for an active drop in a cloud of inactive uniform sized drops was found to be substantially greater than that predicted by Waslo and Gal-Or [17] except at high volume concentration of drops. When the dispersed phase hold up fraction tends to 2/3, the present solution breaks down. If one replaces the size distributed population of drops (or bubbles) by a uniform sized population of drops (or bubbles) of size $\bar{b}_{32}$, the volume surface mean radius of dispersion, the magnitude of possible error in the mass transfer coefficient was found to be less than 6 per cent in all possible cases for the creeping flow regime with no surfactants being present.

NOMENCLATURE

a	Major semiaxes of spheroidal particle (for Chapters 1 to 4)
a	Defined by (5.5) (for Chapters 5 and 6)
A	Defined by (2.54) (for Chapters 1 to 4)
A	Defined by (5.7) (for Chapters 5 and 6)
A_T	Total interfacial area between dispersed phase and continuous phase
b	Minor semiaxes of spheroidal particle (for Chapters 1 to 4)
b	Radius of any drop (for Chapters 5 and 6)
B	Defined by (2.34) (for Chapters 1 to 4)
B	Defined by γ5.8) (for Chapters 5 and 6)
$\bar{b}_3$	Volume average radius of the size distributed dispersion defined by (5.40)
$\bar{b}_{32}$	Volume surface mean radius of the size distributed dispersion defined by (5.27b)
C	Dispersed phase concentration (for Chapters 5 and 6)
C	Defined by (2.1) (for Chapters 1 to 4)
C_1	Defined by (2.13)
C_2	Defined by (2.14)
C_3	Defined by (2.15)
C_i	Concentration of ith species in the fluid
$C_{i\infty}$	Bulk concentration of ith species
C_{i0}	Concentration of ith species at particle surface
D_i	Diffusivity of the ith species
D_e	Distance between the centres of two neighbouring free surface envelopes, defined by (C.4).

E^2 Stokes stream function operator defined by (2.6)

f   Viscosity ratio $(\mu/\bar{\mu})$ (for Chapters 5 and 6)

f   Defined by (2.49a) (for Chapters 1 to 4)

F   Defined by (3.33)

F^* Factor F for prolate spheroidal particle cloud, defined by (3.44)

F_z The force exerted on the body by the fluid in the $\bar{z}$-direction.

g   Defined by (2.7)

G   Defined by (2.17)

G^* Defined by (2.63)

G_∞ Factor G for a particle in an infinite fluid

h   Metrical coefficient defined by (2.43)

h_i Metrical coefficient for ith coordinate (see Happel and Brenner [18])

$\bar{i}_\beta$ Unit vector corresponding to β coordinate

$\bar{i}_\eta$ Unit vector corresponding to η coordinate

$\bar{i}_\varphi$ Unit vector corresponding to φ coordinate

$\bar{\bar{I}}$ Unit tensor

I_b Total diffusional flux to the drop of size b

J   Diffusional flux, defined by (3.22)

k   Bulk or volume viscosity

K   Mass transfer coefficient

K_1, K_2 Integration constants

$\bar{K}_{SD}, \bar{K}_{UD}$ Mass transfer coefficients defined by (5.3), (5.35), (5.44) and (5.46) respectively

K_{SD}, K_{UD}

l_s, l_m Unequal arms of rectangular parellelpiped (see Fig.2)

$n(b)$ Number density distribution of drop radius b

N   Total number of drops per unit volume in the ensemble of drops

$\bar{N}_T$ Total average rate of mass transfer

$\bar{N}_A$ Average rate of mass transfer per unit drop surface area

P   Hydrostatic pressure the fluid would be supporting if it were at rest at its local density and temperature

Pe   Peclet number, $\left(\dfrac{U_s \cdot a}{D_i}\right)$ (for Chapters 1 to 4)

Pe   Peclet number $\left(\dfrac{U_o \cdot 2 \cdot b}{D_i}\right)$ (for Chapters 5 and 6)

P_m Mean normal pressure

r   Distance from the origin of coordinates

Re   Reynolds number, (Ua/ν) (Chapters 1 to 4)

Re   Reynolds number, (Ub/ν) (for Chapters 5 to 6)

$\bar{R}_{SD}, \bar{R}_{UD}$
R_{SD}, R_{UD} Defined by (5.34), (5.37), (5.45) and (5.47) respectively

S   Particle (or drop) surface area

Sch   Schmidt number, (ν/D_i)

Sh   Sherwood number (Ka/D_i) (for Chapters 1 to 4)

Sh   Sherwood number (Kb/D_i) (for Chapters 5 and 6)

U   Ensemble averaged velocity at the location of the test particle before the test particle was added to the cloud velocity of a particle in an infinite fluid (for Chapters 1 to 4)

U_o Ensemble averaged velocity at the location of the test drop before the test drop was added to the cloud value given by (5.6) (for Chapters 5 and 6)

U_s Superficial velocity (for Chapters 1 to 4)

U_s Stokes settling velocity of a solid sphere of density $\overline{\rho}$ defined by (5.9)

v_r Radial component of $\overline{V}$

v_θ Component of $\overline{V}$, in the positive θ direction

$\overline{V}$ Local fluid velocity vector

V_β Radial velocity component defined by (2.41)

V_η Tangential velocity component defined by (2.42)

$\overline{w}$ Defined by (2.1)

W Defined by (5.10)

$\overline{x}$ Cartesian coordinate (See Figure 1)

X Defined by (2.19)

y Nondimensionalised Y defined by (2.55)

$\overline{y}$ Cartesian coordinate (see Figure 1)

Y Normal distance from the particle surface defined by (3.23A)

$\overline{Y}$ Defined by (2.18)

$\overline{z}$ Cartesian coordinate (see Figure 1)

Z Defined by (2.16) (for Chapters 1 to 4)

Z Defined by (5.17) (for Chapters 5 and 6)

GREEK SYMBOLS

$\alpha,$ Defined by (2.3)

α_o Defined by (5.39)

β,η,φ Spheroidal coordinates defined by (2.0) and (2.61A) (See Figure 1).

τ Defined by (2.3)

τ^* Defined by (2.61B)

ψ	Stream function
μ	Dynamic viscosity of continuous phase
$\bar{\mu}$	Dynamic viscosity of dispersed phase
ε	Void fraction defined by (2.74)
$\bar{\varepsilon}$	Void fraction defined by (C.1)
δ	Thickness of the diffusion layer
π	Non dimensionalised concentration of ith species defined by Eq.(3.8)
$\overline{\overline{\Pi}}$	Second rank stress tensor
σ	Defined by (3.15)
ν	Kinematic viscosity
θ	Spherical angle, (Fig. 5)
$\overline{\overline{\Delta}}$	Rate of deformation tensor defined by equation (A.3)
ρ	Density of continuous phase
$\bar{\rho}$	Density of dispersed phase

SUBSCRIPTS

a	Particle surface
b	Solid surface
f	Free surface

SUPERCRIPTS

*	Prolate spheroid
**	Nondimensional quantity
$-$	Vector
$=$	Tensor

CHAPTER 1

INTRODUCTION

In many industrially important operations involving multiphase processing systems, mass is transferred between a large number of solid particles or drops or bubbles moving in a fluid medium and the surrounding fluid. The estimation of mass transfer rate in such systems is quite difficult not only due to the unavailability of velocity profile around a particle or a drop or a bubble in the simplest case but also due to the following features: particle (or drop or bubble) size distribution; the complex geometry (non-spherical) of particles; presence or absence of surfactant impurities in systems with drops or bubbles; residence time distribution etc. Since most of the above features are going to affect the mass transfer rates, a realistic analysis of particulate or dispersed phase systems should incorporate these aspects. Unfortunately, most available analyses avoid these complications by assuming the following: uniform sized particles or drops; particles or drops of spherical shape; constant residence time etc. No analysis is available on the velocity profile and transport rates for shapes other than spherical in particulate systems. The aim of this work is to incorporate some of these features in the analysis of viscous transport in such systems. Specifically, the analysis of fluid dynamics

and mass transport in a cloud of oblate (or prolate) spheroids
has been attempted first since Neale and Nader [1] have
already shown that a realistic model for unconsolidated porous
media or sedimented media or packed beds is provided by a
cloud of oblate (or prolate) spheroids. Chapters 2 to 4 of
this thesis are concerned with this analysis.

Regarding the effect of size distribution, Hoelscher
and Gal-Or [15] had concluded that a size distributed droplet
cloud may be replaced without much error by a cloud of uniform
size droplets of size $\bar{b}_{32}$ which is the volume surface mean
radius of the size distributed cloud. They came to this
conclusion by utilising Levich's [21] expression for mass
transfer coefficient k for a single drop in the flow field for
a size distributed cloud and averaging it over the whole size
distribution. Later Gal-Or and Waslo [16] determined the
velocity profile around a drop for a uniform sized cloud of
drops or bubbles and postulated that these results are valid
for a size distributed system also on the basis of the
conclusions of Hoelscher and Gal-Or [15]. Olney [20] on the
other hand, has shown that the assumption of a uniform drop
size may lead to significant errors in estimates of mass
transfer rates. Therefore, on the basis of Tam's [6] solution
of the flow field for creeping flow around a test sphere placed
in a size distributed cloud of spheres, Sirkar [19] developed
the velocity profile around a test drop in a size distributed

cloud of drops. Such a velocity profile should be used for checking the effect of size distribution on mass transfer rates in a cloud of drops by defining suitable methods of averaging as opposed to the mass transfer rates obtained by Gal-Or and Waslo [17] using Gal-Or and Waslo[16] velocity profiles based on a uniform sized droplet cloud.

The second objective of this work therefore is to determine the mass transfer rates in size distributed cloud of spherical drops or particles using Sirkar [19] and Tam's [6] velocity profiles and Chapters 5 and 6 of this thesis have been devoted to it. This will enable us to check the often used hypothesis 'Replace a size distributed system of spherical particles or drops by a cloud of uniform sized spherical particles or drops having the size equal to the Sauter mean diameter of the size distributed system'. In all of these analyses slow viscous flow is assumed so that creeping flow equations of hydrodynamics are valid. Further high Peclet number is assumed for calculating the mass transport rates so that the concentration boundary layer is affected by velocity in the region close to the solid or drop surface.

CHAPTER 2

HYDRODYNAMICS OF A CLOUD OF OBLATE (OR PROLATE) SPHEROIDAL PARTICLES

Analysis of packed beds and sedimented media encountered in chemical engineering practice require modelling with particles having shape quite different from that of a sphere. Such porous media are necessarily anisotropic. Neale and Nader [1] have recently proposed that such systems may be adequately represented by a homogeneous swarm of aligned particles having the shape of oblate or prolate spheroids. The biophysical problems of transport of oxygen as well as ionic and organic solutes to red blood cells involve transport of the dissolved species to a random suspension of RBC particles. This random suspension of red blood cells has been modelled by Buckles et al. [2], Chilcote [3] and Colton et al.[4] to be a dilute suspension of randomly oriented oblate spheroids. Analysis of transport in porous media or concentrated suspensions with oblate (or prolate) spheroids has an additional advantage in that wide ranging particle shapes between thin circular disks (or slender circular cylinders) and spheres can be accommodated.

Analysis of mass transport rates in creeping flow regime between a fluid and a particle cloud requires the knowledge of the velocity field. There are several models 'cell models' or otherwise, which predict the velocity field around a sphere in a cloud of spheres. The earliest of the

cell models' is due to Cunningham [22] who assumed that each sphere in the cloud would be effectively limited to motion within a concentric fluid mass, the boundary of this outer fluid envelope being solid with no slip at its surface. Cunningham [22] envisaged that this envelope's geometry could be fixed by assuming that either each sphere is within a concentric spherical fluid mass such that the new spheres overlap but only by so much that they just include the whole of the fluid or the arrangement of spherical fluid cells around each particle is such that this fluid spheres are packed in the closest possible arrangement with the fluid in the spaces between them being supposedly occupied by fluid at rest. Obviously due to a certain amount of fluid being at rest in this latter model (model 2), we will obtain a lower limit of the settling velocity whereas with the former model (model 1) an upper limit of the settling velocity is obtained as Cunningham [22] showed, since in terms of relative motion either the outer spherical cell is moving and the inner particle is stationary or vice versa (both being dynamically equivalent). Cunningham [22] preferred the overlapping model (model 1) which is also chosen here but the exact dimensions are to be chosen here on the basis of Hoppel's [5] 'free surface theory' since Happel and Brenner [18] have pointed out (page 387) that in Cunningham's model since the cell volumes are not mutually exclusive, the size of a representative spherical envelope must be fixed by additional empirical consideration'. Hoppel [5] proposed a 'free surface' cell model

in which each sphere in the cloud would be effectively limited
to motion within a concentric mass of fluid such that at this
outer fluid envelope, frictionless flow exists. The fluid envelope
of Happel [5] will be much less than the overlapping fluid
envelope of Cunningham's [22] model 1. In a spherical particle
cloud, any sphere chosen at random would be statistically expected
to be surrounded by a spherically symmetric cluster of spheres.
If the radius of such a particle cluster is assumed to be 2b,
then the vector and scalar profiles will exhibit a maximum or
minimum at a radius b which will be the radius of the free surface.
The radius of the outer solid envelope in Cunningham's model 1
could therefore be 2b, whereas that in Cunningham's model 2 will
be approximately b, the free surface radius. Therefore, as shown
in Figure 1, we assume that,for a cloud of spheroidal particles
with their polar axes parallel to the mean flow, any oblate (or
prolate) spheroid taken at random may be assumed to be surrounded
by a mass of fluid having the shape of the oblate (or prolate)
spheroid and an outer solid surface. Further, this spheroidal fluid
in envelope in model 1 can be geometrically related to a smaller
spheroidal fluid envelope which satisfies the porosity require-
ments of the whole cloud as in Happel's [5] free surface model.
Note that the spheroidal fluid envelope in Cunningham's model 2
essentially coincides with Happel's free surface. Recently Neale
and Nader [1] have modelled practical porous media by means of a
cloud of oblate spheroids in which an oblate spheroid is
surrounded by its associated pore space bounded by a confocal
spheroidal shell with the pore space being determined by overall

porosity of the system. Earlier Jeffrey [10] had calculated
the viscosity of a suspension of ellipsoidal particles by
assuming the ellipsoid to be surrounded by a large sphere.

2.1 Flow Field in a Cloud of Oblate Spheroidal Particles:

This chapter is concerned with the problem of determining
the flow field around an oblate spheroidal particle located
inside a homogeneous cloud of identical oblate spheroidal
particles having a void volume fraction of ε when a fluid
flows past the cloud under conditions of creeping flow. The
mean flow is assumed to be parallel to the polar axis of the
oblate spheroidal particles all of whom are assumed to have
the same orientation. The solution that will be obtained is
also useable for the estimation of the settling velocity of
the ensemble of oblate spheroidal particles if we can assume
that all particles have identical orientation and that the
relative velocity of the fluid with respect to the particle
is equal to the settling velocity of the particle. This last
one however need not be true in the most general case.

The mathematical formulation of this problem is most
appropriately carried out in oblate spheroidal coordinates(β,
η, φ) as shown in Happel and Brenner [18]. The ξ, η and ζ
in Happel and Brenner's [18] nomenclature has been replaced
here by β, τ and α respectively. The oblate spheroid shown
in Figure 1 is defined by

$$\left(\frac{\bar{x}}{a}\right)^2 + \left(\frac{\bar{y}}{a}\right)^2 + \left(\frac{\bar{z}}{b}\right)^2 = 1$$

in cartesian coordinates and the origin of the coordinate system is the instantaneous position of the centre of the oblate spheroid. The cartesian coordinates $(\bar{x}, \bar{y}, \bar{z})$ are related to the oblate spheroidal coordinates β, η and φ by

$$\bar{z} = \sqrt{(a^2-b^2)} \ \text{Sinh} \ \beta \ \text{Cos} \ \eta \tag{2.0}$$

$$\bar{x} = \sqrt{(a^2-b^2)} \ \text{Cosh} \ \beta \ \text{Cos} \ \eta \ \text{Cos} \ \varphi$$

$$\bar{y} = \sqrt{(a^2-b^2)} \ \text{Cosh} \ \beta \ \text{Cos} \ \eta \ \text{Sin} \ \varphi$$

where $\beta \geqslant 0$, $\quad 0 \leqslant \eta \leqslant \pi$, $\quad 0 \leqslant \varphi \leqslant \pi$.

If $c^2 = a^2-b^2$ and $\bar{w}^2 = \bar{x}^2 + \bar{y}^2$ \hfill (2.1)

then β and η are defined by

$$\bar{z} + i \bar{w} = C \ \text{Sinh} \ (\beta + i\eta) \tag{2.2}$$

If we put

$$\tau = \text{Sinh} \ \beta$$

and
$$\alpha = \text{Cos} \ \eta \tag{2.3}$$

the above transformation leads to the relations

$$\bar{z} = C \tau \alpha, \quad \bar{w} = C \sqrt{(\tau^2+1)} \sqrt{(1-\alpha^2)} \tag{2.4}$$

where $0 \leqslant \tau \leqslant \infty$, $\quad -1 \leqslant \alpha \leqslant 1$

It is well known that the solution to the complete Navier-Stokes equations for flows in two and three directions

is very difficult. For flows with constant density and viscosity, however, the differential equations may be somewhat simplified by formulation in terms of a stream function as shown by Happel and Brenner [18]. For creeping motions under steady state conditions, the equations of motion may be expressed in terms of the stream function as

$$E^4 \psi = 0 \tag{2.5}$$

where in oblate spheroidal coordinates the operator E^2 is given as

$$E^2 = \frac{1}{C^2(\tau^2 + \alpha^2)} \left[(\tau^2+1) \frac{\partial^2}{\partial \tau^2} + (1-\alpha^2) \frac{\partial^2}{\partial \alpha^2} \right] \tag{2.6}$$

Happel and Brenner [18] have solved the equation (2.5) for slow fluid motion around an oblate spheroid placed alone in the flow field by considering a trial solution of the form

$$\psi = (1 - \alpha^2)\, g(\tau) \tag{2.7}$$

They obtained the following stream function

$$\psi = (1-\alpha^2) \left[-\frac{1}{2} C_1 \tau + \frac{1}{2} C_2 \tau - \frac{1}{2} C_2 (\tau^2+1) \cot^{-1}\tau \right.$$
$$\left. + C_3(\tau^2+1) \right] \tag{2.8}$$

where C_1, C_2, C_3 are constants which are to be determined from the boundary conditions for the given system.

BOUNDARY CONDITIONS:

As we have considered the oblate spheroidal particles
to be at rest with the fluid streaming past, the following
boundary conditions are valid for flow around any particle
because the normal velocity at surface must be zero:

$$\psi = \quad \text{at} \quad \beta = \beta_a$$
$$\text{or} \quad \tau = \tau_a \quad \text{(Particle surface)} \qquad (2.9)$$

Since the tangential velocity at the particle surface
is also zero, the following condition is obtained:

$$\frac{\partial \psi}{\partial \beta} = 0 \qquad \text{at } \beta = \beta_a \qquad (2.10)$$

or

$$\frac{\partial \psi}{\partial \tau} = 0 \qquad \text{at } \tau = \tau_a \qquad (2.11)$$

(at particle surface)

The assumptions of our model proposed in the introduction
of this chapter would indicate that at the solid surface
bounding the outermost fluid envelope corresponding to $\beta = \beta_b$
shown in Figure 1, the condition of no slip should be valid.
Therefore

$$\psi - \frac{1}{2} U \bar{w}^2 = 0 \qquad \text{at } \beta = \beta_b$$
$$\text{or at } \tau = \tau_b \qquad (2.12)$$

(at solid surface)

Further since this boundary condition is equivalent

to
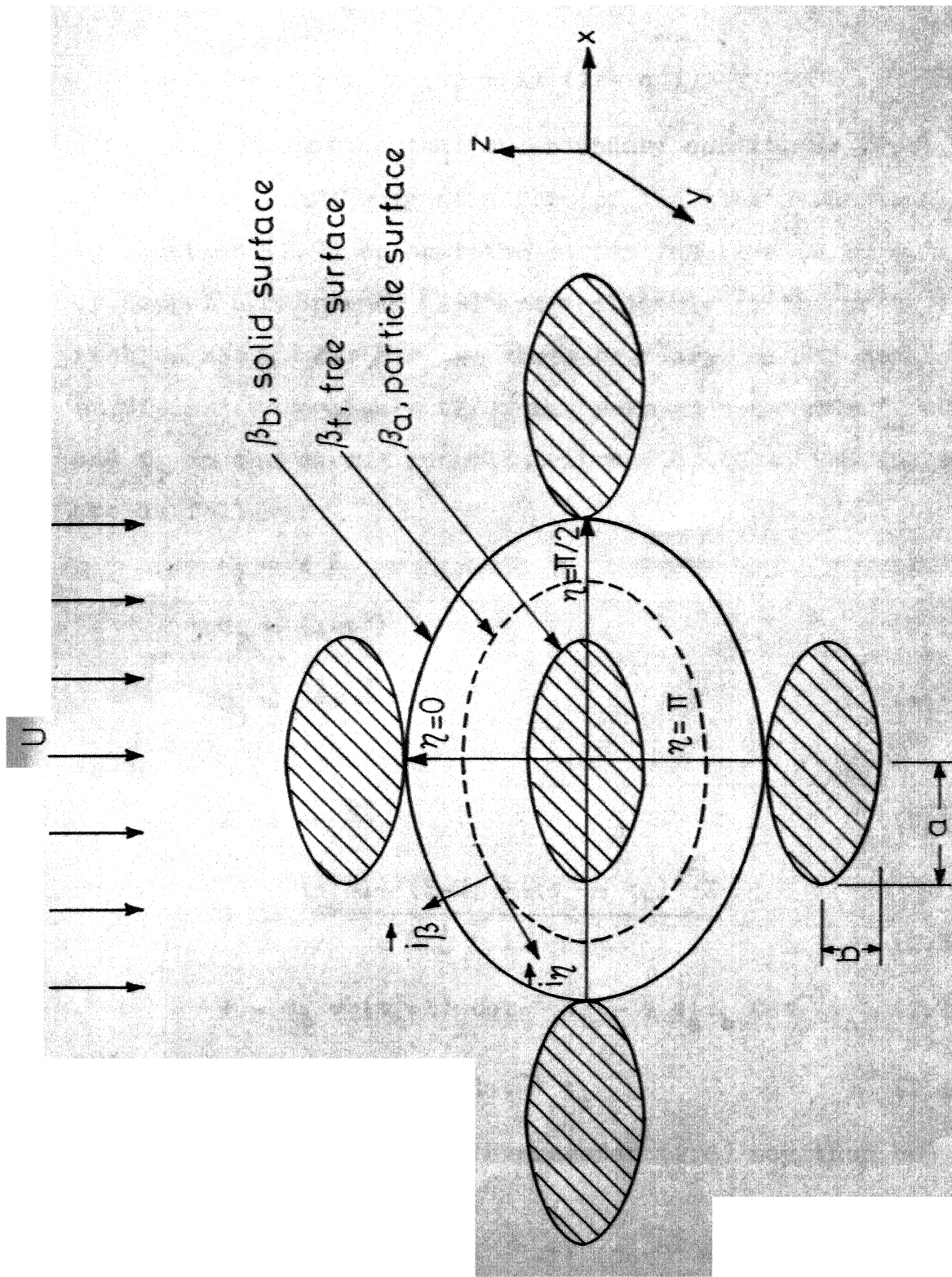
Fig. 1 – Particle locations with respect to fluid flow.

$$\Psi = \frac{1}{2} U C^2 (\tau_b^2 + 1) (1 - \alpha^2)$$

at $\tau = \tau_b$, we notice that the boundary conditions (2.9), (2.11) and (2.12) suggest a form of the stream function given by equation (2.7) so that the stream function (2.8) obtained by Happel and Brenner [18] are applicable to the present problem also. Further the three boundary conditions are sufficient to evaluate the three unknown constants C_1, C_2 and C_3 in the stream function expression (2.8) and their values are as follows:

$$C_1 = 2 Z \tag{2.13}$$

$$C_2 = (1-\tau_a^2) Z \tag{2.14}$$

$$C_3 = \frac{Z X}{2} \tag{2.15}$$

where

$$Z = \frac{U C^2}{G} \tag{2.16}$$

$$G = \frac{(\tau_a^2-1) (Y-X) + (\tau_a - \tau_b)^2 \cdot X}{(\tau_b^2 + 1)} \tag{2.17}$$

$$Y = \tau_b + (\tau_b^2+1) \, \mathrm{Cot}^{-1} \tau_b - 2 \tau_a \tau_b \, \mathrm{Cot}^{-1} \tau_a \tag{2.18}$$

and

$$X = \tau_a - (\tau_a^2-1) \, \mathrm{Cot}^{-1} \tau_a \tag{2.19}$$

The stream function expression (2.8) may then be expressed as

$$\Psi = \frac{1}{2} \frac{U \cdot \overline{w}^2}{G} [\tau_A - (\tau_A^2-1) (\mathrm{Cot}^{-1} \tau_A - \mathrm{Cot}^{-1} \tau) - \frac{\tau \cdot (\tau_a^2 + 1)}{(\tau^2+1)}] \tag{2.20}$$

For the limiting case of only one oblate spheroidal particle in the fluid instead of a cloud of oblate spheroidal particles, we have

$$\tau_b \longrightarrow \infty \qquad \text{which means}$$

$$G = \tau_a - (\tau_a^2 - 1) \, \text{Cot}^{-1} \, \tau_a \qquad (2.21)$$

and the stream function expression (2.20) reduces to (See Appendix B equations from B.1 to B.5)

$$\psi = \frac{1}{2} U \, \bar{w}^2 \left[1 - \frac{\left(\dfrac{\tau}{\tau^2+1}\right) - \left(\dfrac{\tau_a^2-1}{\tau_a^2+1}\right) \text{Cot}^{-1} \, \tau}{\left(\dfrac{\tau_a}{\tau_a^2+1}\right) - \left(\dfrac{\tau_a^2-1}{\tau_a^2+1}\right) \text{Cot}^{-1} \tau_a} \right] \qquad (2.22)$$

which is identical to the stream function for flow around a single oblate spheroidal particle as derived by Happel and Brenner [18].

2.2 Drag on a Oblate Spheroidal Particle Placed Inside a Cloud of Identical Particles:

The most general expression (which is derived in Appendix A) for the force exerted on an axially symmetric solid particle, bubble or drop by the fluid in the direction of the mean fluid flow is

$$F_z = \pi \mu \oint \bar{w}^3 \, \frac{\partial}{\partial \beta} \left[\frac{E^2 \psi}{\bar{w}^2} \right] \delta \eta$$

$$- 2\pi \mu \oint h \, \frac{\partial \psi}{\partial \beta} \left[\frac{\partial \bar{w}}{\partial \beta} \, \frac{\partial h}{\partial \beta} + \frac{\partial \bar{w}}{\partial \eta} \, \frac{\partial h}{\partial \eta} \right] \delta \eta \qquad (2.23)$$

The integrals are over the whole surface of the axially symmetric solid particle, drop or bubble. For an axially symmetric solid particle the second integral term will vanish because at the solid surface,

$$\frac{\partial \psi}{\partial \beta} \Bigg|_{\text{particle surface}} = 0 \qquad \text{(boundary condition(2.10))}$$

Thus for a axially symmetric solid particle, the drag force expression (2.23) reduces to

$$F_z = \pi \mu \int \bar{w}^3 \frac{\partial}{\partial \beta} \left[\frac{E^2 \psi}{\bar{w}^2} \right] \delta \eta \qquad (2.24)$$

which is available in Happel and Brenner [18].

For the sake of convenience, we replace β and η in this equation by equations (2.3) so that the drag expression (2.24) for an oblate spheroidal particle is given by

$$F_z = -\pi\mu \int_{-1}^{1} \frac{\bar{w}^3 \sqrt{(\tau_a^2+1)}}{\sqrt{(1-\alpha^2)}} \frac{\partial}{\partial \tau} \left[\frac{E^2 \psi}{\bar{w}^2} \right]_{\text{at } \tau=\tau_a} d\alpha \qquad (2.25)$$

where the operator E^2, ψ and $\bar{w}$ are defined by the equations (2.6), (2.20) and (2.4) respectively. Now

$$E^2 \psi = \frac{1}{c^2(\tau^2+\alpha^2)} \left[(\tau^2+1) \frac{\partial^2 \psi}{\partial \tau^2} + (1-\alpha^2) \frac{\partial^2 \psi}{\partial \alpha^2} \right] \qquad (2.26)$$

which on simplification reduces to the following expression:

$$E^2 \psi = \frac{C_1 (1-\alpha^2) \tau}{c^2 (\tau^2+\alpha^2)} \qquad (2.27)$$

By (2.4) and (2.27) we get

$$\frac{\partial}{\partial \tau} \left[\frac{E^2 \psi}{\bar{w}^2} \right]_{at \ \tau=\tau_a} = \frac{C_1}{C^4} \left[\frac{(\tau_a^2+\alpha^2)(\tau_a^2+1)-2\tau_a^2(2\tau_a^2+\alpha^2+1)}{(\tau_a^2+\alpha^2)(\tau_a^2+1)^2} \right]$$

(2.28)

Substitution of (2.28) into (2.25) leads to the following drag expression

$$F_z = - \frac{\pi \mu C_1}{C} \int_{-1}^{1} \frac{(1-\alpha^2)}{(\tau_a^2+\alpha^2)^2} [(\tau_a^2+\alpha^2)(\tau_a^2+1)$$

$$-2\tau_a^2(1+2\tau_a^2+\alpha^2)]d\alpha$$

(2.29)

or

$$F_z = - \frac{2\pi \mu C_1}{C} \left[(\tau_a^2-1) - \frac{(1+\tau_a^2)^2}{2\tau_a} \ Sin(2 \ Cot^{-1} \ \tau_a) \right]$$

(2.30)

where C_1 is defined by (2.13) and reduces to the following on using (2.16):

$$C_1 = \frac{2 \ U \ C^2}{G}$$

(2.31)

Here G is defined by (2.17) and is also equal to the following:

$$G = Sinh \ \beta_a + (Sinh^2 \ \beta_a - 1)[Cot^{-1} \ Sinh \ \beta_b - Cot^{-1} \ Sinh \ \beta_a]$$

$$- \frac{Sinh \ \beta_b}{Cosh^2 \ \beta_b} \ Cosh^2 \ \beta_a$$

(2.32)

Further U may be considered as the ensemble averaged velocity of the particle cloud if the cloud were settling :

in the fluid. For a fixed particle cloud with fluid moving around it,

$$F_z = \frac{4 \pi \mu U C (1+B)}{G} \tag{2.33}$$

where

$$B = \frac{\cosh^4 \beta_a}{2 \sinh \beta_a} \sin(2 \cot^{-1} \sinh \beta_a) - \sinh^2 \beta_a \tag{2.34}$$

or

$$B = 1.0 \tag{2.35}$$

Thus

$$F_z = \frac{8 \pi \mu U C}{G} \tag{2.36}$$

For the limiting case of only one oblate spheroidal particle in the fluid instead of a cloud of oblate spheroidal particles we have

$$\tau_b \longrightarrow \infty \qquad \text{which means}$$

$$G_\infty = G \Big|_{\tau_b = \infty} = \tau_a - (\tau_a^2 - 1)(\cot^{-1} \tau_a) \tag{2.37}$$

and the drag force expression (2.36) reduces to

$$F_z = \frac{8 \pi \mu U C}{\tau_a - (\tau_a^2 - 1) \cot^{-1} \tau_a} \tag{2.38}$$

which is identical to the drag force expression for a single oblate spheroidal particle as derived by Happel and Brenner [18].

Expression (2.36) also reduces to the well known
Stokes' law of resistance for the limiting case of a single
sphere in a moving fluid in the creeping flow regime as shown
in Appendix B equations (B.5 and B.6).

2.3 Ensemble Averaged Velocity:

We have assumed earlier that the inner oblate spheroidal
particle is at rest while the outer oblate spheroidal fluid
envelope moves with an ensemble averaged velocity U. This
problem is identical to that of an inner oblate spheroidal
particle moving with velocity U at the center of a stationary
outer oblate spheroidal fluid envelope. Thus the drag force
experienced by the single oblate spheroidal particle will be
same in both the situations, i.e.

$$F_z = - \frac{8 \pi \mu U C}{G} \qquad (2.36)$$

where the oblate spheroidal particle is moving in a direction
opposite to that in which the fluid was moving when the particles
were at rest.

Let an oblate spheroidal particle moving with velocity
U_o in an infinite medium experience the same force F_z experienced
by the same oblate spheroidal particle when moving with an
ensemble averaged velocity U in a cloud of particles. Now
for a single oblate spheroid F_z and U_o are related by

$$F_z = \frac{8 \pi \mu U_0 C}{G_{\tau_b=\infty}} \qquad (2.39)$$

Using (2.36), (2.37) and (2.39) we can obtain the ensemble averaged velocity U in a particle cloud as

$$\frac{U}{U_0} = \frac{\text{Sinh } \beta_a + (\text{Sinh}^2\beta_a - 1)[\text{Cot}^{-1}\text{Sinh } \beta_b - \text{Cot}^{-1}\text{Sinh } \beta_a] - \dfrac{\text{Sinh } \beta_b}{\text{Cosh}^2 \beta_b} \text{Cosh}^2 \beta_a}{\text{Sinh } \beta_a - (\text{Sinh}^2 \beta_a - 1) \text{Cot}^{-1} \text{Sinh } \beta_a} \qquad (2.40)$$

2.4 Velocity Profile Near the Surface of an Oblate Spheroidal Particle Placed in a Cloud of Similar Particles:

In scalar transport at high Schmidt or Prandtl numbers, the scalar transport is confined to a region very close to the solid surface over which the fluid is flowing. The solutions of convective scalar transport equations require velocity profile close to the solid surface. In this section we propose to determine the velocity profile near the surface of an oblate spheroidal particle placed in a cloud of similar particles.

The following relations exist between the radial and tangential velocity components and the stream function for any axisymmetric body with orthogonal curvilinear coordinates β, η, φ (Figure 1):

$$V_\beta = -\frac{h_\eta}{w} \frac{\partial \psi}{\partial \eta} \qquad (2.41)$$

and

$$V_\eta = \frac{h_\beta}{\bar{w}} \frac{\partial \psi}{\partial \beta} \qquad (2.42)$$

For an oblate spheroid h_β, h_η and $\bar{w}$ are defined as follows:

(Happel and Brenner [18] Page 515)

$$h = h_\beta = h_\eta = \frac{1}{C\sqrt{(\cosh^2\beta - \sin^2\eta)}} \qquad (2.43)$$

and

$$\bar{w} = \frac{1}{h_\varphi} = C \cosh\beta \, \sin\eta \qquad (2.44)$$

The β coordinate of any point in the fluid close to the surface of the oblate spheroid defined /by the coordinate β_a can be expressed as

$$\beta = \beta_a + \triangle\beta \qquad (2.45)$$

For locations close enough to the surface of oblate spheroid, $\triangle\beta$ may be considered to be negligibly small compared β_a so that one can approximate

$$h_\beta(\beta,\eta) \approx h_{\beta_a}(\beta_a, \eta) \qquad (2.46A)$$

and

$$h_\varphi(\beta,\eta) \approx h_\varphi(\beta_a,\eta) \qquad (2.46B)$$

Therefore

$$h = h_\beta \approx h_{\beta_a} = \frac{1}{C\sqrt{(\cosh^2\beta_a - \sin^2\eta)}} \qquad (2.46C)$$

and

$$h_\varphi \approx \frac{1}{C \, \text{Cosh} \, \beta_a \, \text{Sin} \, \eta} \qquad (2.46D)$$

The expression (2.42) may be written in the following form

$$V_\eta = \frac{h_\beta}{\bar{w}} \, \frac{\partial \psi}{\partial \tau} \, \frac{d \tau}{d \beta} \qquad (2.47)$$

Substitution of h_β, $\bar{w}$, $\frac{\partial \psi}{\partial \tau}$ and $\frac{d \tau}{d \beta}$ from (2.46C), (2.44), (2.8) and (2.3) in (2.47) lead to the following expression

$$V_\eta = \frac{\text{Sin} \, \eta}{C^2 \sqrt{(\text{Cosh}^2 \beta_a - \text{Sin}^2 \eta)}} [- \frac{C_1}{2} + C_2(1 - \tau \, \text{Cot}^{-1} \, \tau) + 2 \, C_3 \, \tau \,] \qquad (2.48)$$

or

$$V_\eta = \frac{\text{Sin} \, \eta}{C^2 \sqrt{(\text{Cosh}^2 \beta_a - \text{Sin}^2 \eta)}} [- \frac{C_1}{2} + C_2 - C_2 \, \text{Sin} \, \beta \, \text{Cot}^{-1} \, \text{Sinh} \, \beta + 2 \, C_3 \, \text{Sinh} \, \beta] \qquad (2.49)$$

Since $\beta = \beta_a + \triangle \beta$, a function of β may be expanded in Taylor's series around the value of the function at β_a as

$$f(\beta) = f(\beta_a) + \triangle \beta \, f'(\beta_a) + \frac{(\triangle \beta)^2}{2!} \, f''(\beta_a) + \ldots \ldots + \ldots \ldots \qquad (2.49a)$$

As $\triangle \beta$ is very small, we can neglect terms having $(\triangle \beta)^2$ or higher powers of $\triangle \beta$ in comparison with terms containing $\triangle \beta$ thus

$$f(\beta) = f(\beta_a) + \triangle \beta \, f'(\beta_a) \qquad (2.50)$$

This leads to

$$\text{Sinh } \beta = \text{Sinh } (\beta_a + \triangle\beta)$$

$$= \text{Sinh } \beta_a + \triangle\beta \text{ Cosh } \beta_a \qquad (2.51)$$

and

$$\text{Sinh } \beta \text{ Cot}^{-1} \text{ Sinh } \beta = \text{Sinh } (\beta_a + \triangle\beta) \text{ Cot}^{-1} \text{ Sinh } (\beta_a + \triangle\beta)$$

$$= \text{Sinh } \beta_a \text{ Cot}^{-1} \text{ Sinh } \beta_a + \triangle\beta \text{ (Cosh } \beta_a \text{ Cot}^{-1} \text{ Sinh } \beta_a$$

$$- \text{ Tanh } \beta_a) \qquad (2.52)$$

By substituting C_1, C_2, C_3 from (2.13), (2.14) and (2.15) respectively into (2.49) and using (2.51) and (2.52), the expression (2.49) reduces to

$$V_\eta = \frac{A \text{ Sin } \eta}{\sqrt{(\text{Cosh}^2 \beta_a - \text{Sin}^2\eta)}} \triangle\beta \qquad (2.53)$$

where

$$A = \frac{2 U \text{ Tanh } \beta_a}{G} \qquad (2.54)$$

and G is defined by expression (2.33).

Now if we define

$$y = \triangle\beta = \beta - \beta_a \qquad (2.55)$$

we obtain

$$V_\eta = \frac{A \text{ Sin } \eta}{\sqrt{(\text{Cosh}^2 \beta_a - \text{Sinh}^2\eta)}} y \qquad (2.56)$$

The radial velocity component V_β may be determined either by equation (2.41) or by substituting (2.56) into the continuity equation. The latter approach is easier.

The continuity equation is

or
$$\nabla \cdot \vec{V} = 0$$

$$\frac{\partial}{\partial \beta} \left(\frac{V_\beta}{h_\eta \, h_\varphi} \right) + \frac{\partial}{\partial \eta} \left(\frac{V_\eta}{h_\beta \, h_\varphi} \right) = 0 \tag{2.57}$$

or

$$\frac{\partial}{\partial \beta} \left(\frac{V_\beta}{h_\eta \, h_\varphi} \right) = - \frac{\partial}{\partial \eta} \left(\frac{V_\eta}{h_\varphi \, h_\beta} \right)$$

Using (2.56), (2.46C) and (2.46D)

$$\frac{\partial}{\partial \beta} \left(\frac{V_\beta}{h_\eta \, h_\varphi} \right) = -2C^2 \, A \, \text{Cosh} \, \beta_a \left(\text{Sin}^2 \eta \right) y$$

or

$$\frac{\partial}{\partial y} \left(\frac{V_\beta}{h_\eta \, h_\varphi} \right) = -2C^2 \, A \, \text{Cosh} \, \beta_a \left(\text{Sin}^2 \eta \right) y$$

or

$$\frac{V_\beta}{h_\eta \, h_\varphi} = -C^2 A \, \text{Cosh} \, \beta_a \left(\text{Sin}^2 \, \eta \right) y^2 + K_1$$

where K_1 is a constant of integration and equal to zero because
at y=0

$$V_\beta = 0$$

Thus

$$V_\beta = -A \cdot C^2 \, h_\eta \cdot h_\varphi \, \text{Cosh} \, \beta_a \left(\text{Sin}^2 \eta \right) y$$

By relations (2.46C) and (2.46D) we can rearrange the
above to

$$V_\beta = - \frac{A \, \text{Cos} \eta \; y^2}{\sqrt{(\text{Cosh}^2 \, \beta_a - \text{Sin}^2 \eta)}} \tag{2.58}$$

By using expression (2.54) in (2.56) and (2.58) the radial and tangential velocity components may be expressed as follows:

Radial component:

$$V_\beta = - \frac{2U \; \text{Tanh} \; \beta_a \cdot \text{Cos} \eta \cdot y^2}{G\sqrt{(\text{Cosh}^2 \beta_a - \text{Sin}^2 \eta)}} \qquad (2.59)$$

Tangential component:

$$V_\eta = \frac{2U \; \text{Tanh} \; \beta_a \cdot \text{Sin} \eta \; y}{G\sqrt{(\text{Cosh}^2 \beta_a - \text{Sin}^2 \eta)}} \qquad (2.60)$$

2.5 Expressions for a Cloud of Prolate Spheroidal Particles:

The prolate spheroid is defined by

$$(\frac{\bar{x}}{b})^2 + (\frac{\bar{y}}{b})^2 + (\frac{\bar{z}}{a})^2 = 1 \qquad (2.61)$$

The coordinates β and η are defined by

$$(\bar{z} + i \; \bar{w}^*) = C \; \text{Cosh} \; (\beta + i\eta) \qquad (2.61A)$$

where

$$C = \sqrt{(a^2 - b^2)}$$

$$\bar{w}^* = \sqrt{(\bar{x}^2 + \bar{y}^2)}$$

If we put

$$\tau^* = \text{Cosh} \beta \quad \text{and} \quad \alpha = \text{Cos} \eta \qquad (2.61b)$$

the above transformation leads to the relations

$$\bar{z} = C \; \tau^* \; \alpha \quad \text{and} \quad \bar{w}^* = C\sqrt{((\tau^{*2} - 1))} \; \sqrt{(1 - \alpha^2)} \qquad (2.61C)$$

where $\; 0 \leq \tau^* \leq \infty \qquad$ and $\qquad -1 \leq \alpha \leq 1$

All expressions which have been derived for an oblate spheroidal particle cloud in Sections 2.1, 2.2, 2.3 and 2.4, can also be derived for a prolate spheroidal particle cloud by methods very similar to those employed for oblate spheroidal particles in the above mentioned sections. Instead of considering the new problem separately, all the expressions for prolate spheroidal cloud can therefore be obtained from the analogous results for an oblate spheroidal cloud by a simple transformation to imaginary values of parameters and coordinates. For example, by replacing τ^* by $i\tau$ and C by $-iC$ in equation (2.20) [18], the stream function for flow around a prolate spheroidal particle placed in a cloud of prolate spheroidal particles may be expressed as

$$\psi^* = \frac{U^* \bar{w}^{*2}}{2\, G^*} \left[\tau_a^* - (\tau_a^{*2} + 1)(\operatorname{Cot} h^{-1} \tau_a^* - \operatorname{Coth}^{-1} \tau^*) - \frac{\tau^*(1 - \tau_a^{*2})}{(1 - \tau^{*2})} \right] \qquad (2.62)$$

where

$$G^* = \frac{(\tau_a^{*2} + 1)(Y^* - X^*) + (\tau_a^* - \tau_b^*)^2 X^*}{(\tau_b^{*2} - 1)} \qquad (2.63)$$

or

$$G^* = \frac{\operatorname{Cosh} \beta_b}{\operatorname{Sinh}^2 \beta_b} \operatorname{Sinh}^2 \beta_a + (\operatorname{Cosh}^2 \beta_a + 1)(\operatorname{Coth}^{-1} \operatorname{Cos}\beta_a - \operatorname{Coth}^{-1} \operatorname{Cosh}\beta_b) - \operatorname{Cosh} \beta_a \qquad (2.64)$$

$$Y^* = \tau_b^* + (\tau_b^{*2} - 1)\operatorname{Coth}^{-1} \tau_b^* - 2\, \tau_a^* \tau_b^* \operatorname{Coth}^{-1} \tau_o^* \qquad (2.65)$$

$$X^* = \tau_a^* - (\tau_a^{*2}+1) \; Coth^{-1} \; \tau_a^* \tag{2.66}$$

and

$$\bar{w}^* = C\sqrt{((\tau_a^{*2} - 1))} \cdot \sqrt{(1-\alpha^2)} \tag{2.67}$$

For the limiting case of flow around a single prolate spheroidal particle in an infinite fluid medium, we have

$$\tau_b^* \longrightarrow \infty$$

and the expression (2.62) reduces to the result obtained by Happel and Brenner [18] (Page 155).

By a similar transformation, the drag expression (2.36) and the expressions for the ensemble averaged velocity (2.40), the radial velocity (2.59) and the tangential velocity (2.60) for a oblate spheroidal particle cloud may also be transformed to the following expressions for a prolate spheroidal particle cloud

$$F_z^* = \frac{8\pi\mu U^* C}{G^*} \tag{2.68}$$

$$\frac{U^*}{U_0^*} = \frac{\begin{array}{c} Cosh\,\beta_a - (1+Cosh^2\beta_a)[\,Coth^{-1}\,Cosh\beta_a - Coth^{-1}Cos\beta_b\,] \\ - \dfrac{Cosh\,\beta_b}{Sinh^2\beta_b} Sinh^2\,\beta_a \end{array}}{Cosh\,\beta_a - (1+Cosh^2\beta_a)\,Coth^{-1}\,Cosh\,\beta_a} \tag{2.69}$$

$$V_\beta^* = - \frac{2U^* Coth\,\beta_a\,Cos\eta\,y^2}{G^* \sqrt{(Sinh^2\,\beta_a + Sin^2\eta)}} \tag{2.70}$$

and

$$V_\eta^* = \frac{2U^* \, \text{Coth} \, \beta_a \left(\text{Sin}\eta\right)y}{G^* \sqrt{(\text{Sinh}^2\beta_a + \text{Sin}^2\eta)}} \qquad (3.71)$$

When $\tau_b^* \longrightarrow \infty$, expression (2.68) for the drag reduces to the result obtained by Happel and Brenner [18] (page 155) for drag on a single prolate spheroid. Expression (2.68) becomes the Stoke\$s law of resistance for a sphere when

$$\tau_b^* \longrightarrow \infty \qquad \text{and} \qquad \tau_a^* \longrightarrow \infty$$

By the proposed model, we have thus been able to determine the following quantities describing the viscous fluid dynamics in a cloud of oblate (or prolate) spheroids:

(i) stream function

(ii) drag force on an oblate (or prolate) spheroid in a cloud

(iii) Ensemble averaged velocity

(iv) Velocity profile close to the surface of oblate (or prolate) spheroidal particle.

It must be pointed out however that this is the first attempt of this kind for a cloud of oblate spheroidal particles. The effects of orientation of the particles around the assumed mean position is unknown. Further the difference in the requirements of analysis for a cloud of fixed particles or free particles has not been considered here [23]. We have considered only cell models in the

derivations presented here as well as in the literature reviewed for the objectives of this work.

2.6 Relationship of Outer Solid Envelope and Free Surface with Void Fraction ε:

The average void volume fraction ε is defined as the ratio of the total volume of fluid to the total volume of the assemblage. It is implicit in such an assumption that the statistical average distance between any two neighbouring particles in a cloud of particles will be a direct function of the void fraction. As ε is increased, the average interparticular distance will increase. In the model proposed in the introduction of this chapter, the normal distance between the particle surface and the outer solid envelope of the cell fluid surrounding the particle is directly related to the statistical average distance between any two neighbouring particles in the cloud. If this normal distance is Y_{SP} then one can approximate the normal distance between the free surface and the particle surface by $Y_{FP} = Y_{SP}/2$. Thus

$$Y_{FP} = Y_{SF} = Y_{SP}/2 \tag{2.72}$$

where Y_{ij} - is the normal distance between ith and jth spheroidal surfaces with the former enclosing the latter.

Equations (2.72) with (3.23 A) gives the relation between the outer solid envelope, the free surface of Happel[5]

and the particle surface in the proposed model. The relation may be deduced as

$$\text{Sinh } \beta_b - \text{Sinh } \beta_f = \text{Sinh } \beta_f - \text{Sinh } \beta_a$$

or

$$\text{Sinh } \beta_b = 2 \text{ Sinh } \beta_f - \text{Sinh } \beta_a \qquad (2.73)$$

To determine β_f, we assume following Happel [5] that the void fraction for the free surface - particle cell is equal to the overall average void fraction in the particle assemblage with each free surface effectively isolating each particle.

Thus

$$(1-\epsilon) = \frac{\text{Volume of one particle}}{\text{Volume within each free surface}}$$
$$(2.74)$$

This leads to

(i)   for an assemblage of oblate spheroidal particles of dimension β_a (See Neale and Nader [1]).

$$\text{Sinh } \beta_f \text{ Cosh}^2\beta_f = \frac{\text{Sinh } \beta_a \text{ Cosh}^2\beta_a}{(1-\epsilon)} \qquad (2.75A)$$

(ii)   and for an assemblage of prolate spheroidal particles (see Neale and Nader [1])

$$\text{Sinh}^2\beta_f \text{ Cosh } \beta_f = \frac{\text{Sinh}^2\beta_a \text{ Cosh } \beta_a}{(1-\epsilon)} \qquad (2.75B)$$

The appropriate value of β_a is uniquely defined in terms of the basic dimensions of the spheroid a (semi major axis) and b (semi minor axis). i.e.

$$\text{Cosh } \beta_a = \frac{1}{\sqrt{(1 - (\frac{b}{a})^2)}} \tag{2.76}$$

Thus the equations (2.73), (2.75) and (2.76) provide the necessary relationship between β_b and the void fraction ϵ of the assemblage of an oblate (or prolate) spheroidal particles having a particular value of the eccentricity (b/a) of the spheroid. The above dealt with model 1 of Cunningham adopted here. However in case of model 2 of Cunningham, the free surface of dimension β_f will replace β_b so that for a given ϵ, from equation (2.75A) or (2.75B), β_f is known. This β_f will then replace β_b in all the expressions derived in sections 2.1, 2.2, 2.3, 2.4 and 2.5.

2.7 Velocity Profile Around a Particle at $\eta = \pi/2$ Location:

In section 2.4 we developed the expressions for linearized radial and tangential velocity components around a particle placed in a cloud of identical particles. In fact those expressions will predict the corresponding velocities without any significant error only near the particle surface. In this section we propose to determine the actual velocity profile around a particle at the radial location $\eta = \pi/2$.

From equation (2.41)

$$V_\beta = -\frac{h_\pi}{\overline{w}} \frac{\partial \psi}{\partial \eta} \tag{2.77}$$
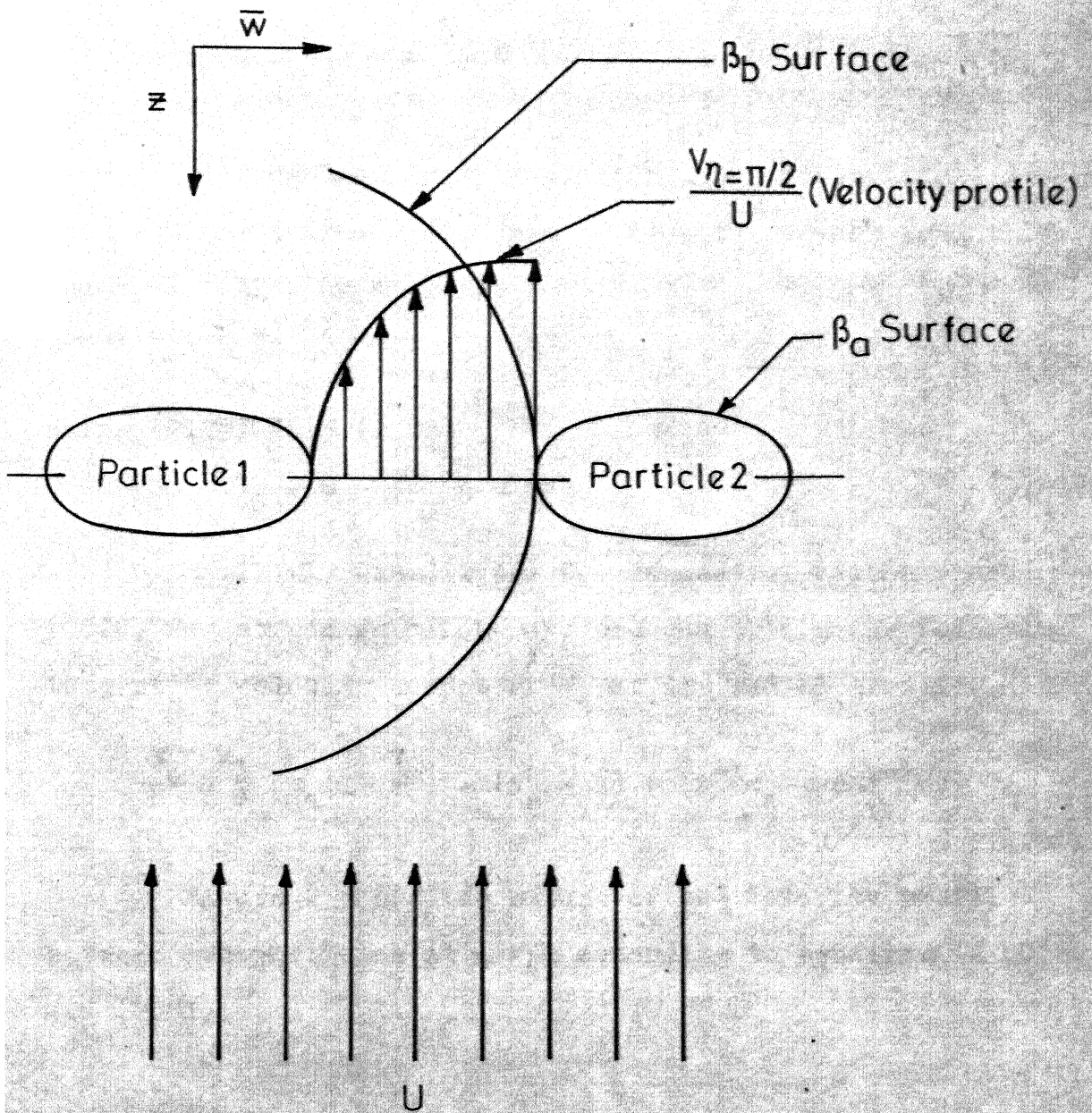
Fig. 2 – Expected velocity profile between two particles.

or

$$V_\beta = -\frac{h_\eta}{\bar{w}} \frac{\partial \Psi}{\partial \bar{w}} \frac{\partial \bar{w}}{\partial \eta} \qquad (2.78)$$

Differentiating the relation which comes after substituting α from (2.3) into (2.4) with respect to η which leads to following at $\eta = \pi/2$

$$\frac{\partial \bar{w}}{\partial \eta} = 0 \qquad (2.79)$$

using (2.79) into (2.78)

$$V_\beta = 0 \qquad \text{at } \eta = \pi/2 \qquad (2.80)$$

Similarly from (2.42) for tangential velocity and (2.20) for stream function Ψ, one can obtain the following tangential velocity component V_η at the radial location $\eta = \pi/2$.

$$\frac{V_\eta}{U} = \frac{1}{G} \left[\tau_a (1 - \frac{\tau_a}{\tau}) - (\tau_a^2 - 1)(\cot^{-1}\tau_a - \cot^{-1}\tau) \right] \qquad (2.81)$$

Figure 2 shows the nature of the velocity profile between two particles at $\eta = \pi/2$ according to equation (2 80) and (2.81).

CHAPTER 3

MASS TRANSFER TO A SINGLE ACTIVE OBLATE SPHEROIDAL PARTICLE IN A CLOUD OF INACTIVE IDENTICAL OBLATE SPHEROIDAL PARTICLES AT HIGH SCHMIDT NUMBERS

For large Schmidt numbers in the creeping flow regime, Pfeffer [11] had analytically determined the Sherwood number for a spherical active particle as a function of the Peclet number and the fractional void volume in a cloud of uniform spherical inactive particles by using the velocity profile derived from the 'free surface model' of Happel [5]. For a random cloud of size distributed spherical particles, Sirkar [12] obtained an analytical relationship between the Sherwood number of an active particle, the Peclet number, the fractional void volume and the size distribution function by approximating the velocity profile of Tam [6] close to the solid surface. The problem of mass transport to a non-spherical particle in a cloud of non-spherical particles has not, however, received enough attention. Lightfoot [13] on the basis of Stewart's work [14] has indicated the formalism to be adopted for obtaining the Sherwood number for mass transfer to a single particle of complex geometry placed alone in the flow field at high Schmidt numbers. Using the velocity profile around an oblate spheroid in a cloud of oblate spheroids, which has been derived in the previous chapter, and Lightfoot's mass

transport analysis for an isolated particle with smooth but complex spheroidal geometry an analytical solution of mass transport to an oblate (or prolate) spheroid in a cloud of oblate (or prolate) spheroids has been carried out in this chapter.

3.1 Convective Diffusion to an Oblate Spheroidal Particle:

The equation which is applicable for the convective diffusion of species i from or to the surface of the particle under conditions of constant density and diffusivity (at const constant temperature and pressure) is

$$\frac{\partial c_i}{\partial t} + (\bar{v} \cdot \nabla c_i) = D_i \nabla^2 \cdot c_i + R_i$$

$$\underset{\longrightarrow 0}{\text{Steady State}} \qquad\qquad \underset{\longrightarrow 0}{\text{No Chemical Reaction}}$$

or

$$(\bar{v} \cdot \nabla c_i) = D_i \nabla^2 \cdot c_i \qquad\qquad (3.1)$$

The equation for convective diffusion of species i takes the following form in the coordinate system adopted in Chapter 2:

$$\frac{1}{D_i} \left[\frac{v_\beta}{h_\eta} \frac{\partial c_i}{\partial \beta} + \frac{v_\eta}{h_\beta} \frac{\partial c_i}{\partial \eta} \right] = \frac{\partial^2 c_i}{\partial \beta^2} + \frac{\partial^2 c_i}{\partial \eta^2} \qquad (3.2)$$

A comparison of the magnitude of the various terms in the equation (3.2) for conditions close to the surface

so that $\beta = \beta_a + \delta$ where δ is the thickness of the diffusion layer leads to the following (on the basis of similar approximations by Levich [21]

$$\frac{\partial c_i}{\partial \eta} \approx \frac{\Delta c_i}{2b}$$

$$\frac{\partial^2 c_i}{\partial \eta^2} \approx \frac{\Delta c_i}{4 b^2} \qquad (3.3)$$

and

$$\frac{\partial c_i}{\partial \beta} \approx \frac{\Delta c_i}{\delta}$$

$$\frac{\partial^2 c_i}{\partial \beta^2} \approx \frac{\Delta c_i}{\delta^2} \qquad (3.4)$$

Further $\delta \ll b$ (which is the semi-minor axis for an oblate spheroid) for the condition of high Schmidt numbers. Hence

$$\frac{\partial^2 c_i}{\partial \beta^2} \gg \frac{\partial^2 c_i}{\partial \eta^2} \qquad (3.5)$$

as has been shown by Levich [21] for a sphere.

Thus equation (3.2) becomes

$$\frac{1}{D_i} \left[\frac{V_\beta}{h_\eta} \frac{\partial c_i}{\partial \beta} + \frac{V_\eta}{h_\beta} \frac{\partial c_i}{\partial \eta} \right] = \frac{\partial^2 c_i}{\partial \beta^2} \qquad (3.6)$$

The equation (3.6) in dimensionless variables may be written as follows:

$$\frac{U}{D_i h} \left[V_\beta^{**} \frac{\partial \bar{\pi}}{\partial \beta} + V_\eta^{**} \frac{\partial \bar{\pi}}{\partial \eta} \right] = \frac{\partial^2 \bar{\pi}}{\partial \beta^2} \qquad (3.7)$$

where

$$\overline{\pi} = \frac{C_i - C_{io}}{C_i - C_{io}} \tag{3.8}$$

$$h = h_\beta = h_\eta \tag{2.43}$$

$$V_\beta^{**} = \frac{V_\beta}{U} \tag{3.9}$$

$$V_\eta^{**} = \frac{V_\eta}{U}$$

By (2.55), (2.59) and (2.60), the following relations may be used:

$$\frac{\partial}{\partial \beta} = \frac{\partial}{\partial y} \tag{3.10}$$

$$V_\beta^{**} = \frac{V_\beta}{U} = - \frac{2 \; \text{Tanh} \; \beta_a \; \text{Cos}\eta \; y^2}{G\sqrt{(\text{Cosh}^2 \; \beta_a - \text{Sin}^2 \eta)}} = -K \; \text{Cos}\eta \cdot y^2 \tag{3.11}$$

$$V_\eta^{**} = \frac{V_\eta}{U} = \frac{2 \; \text{Tanh} \; \beta_a \; \text{Sin}\eta \; y}{G\sqrt{(\text{Cosh}^2 \beta_a - \text{Sin}^2 \eta)}} = K \; \text{Sin}\eta \; y \tag{3.12}$$

where $\quad K = \dfrac{2 \; \text{Tanh} \; \beta_a}{G\sqrt{(\text{Cosh}^2\beta_a - \text{Sin}^2 \eta)}}$ \tag{3.12A}

By substituting (3.10), (3.11), (3.12) and (2.46A) into equation (3.7), we obtain the following

$$\text{Re} \cdot \text{Sch} \; \sqrt{\left[1 - \left(\frac{\text{Sin}\eta}{\text{Cosh}\beta_a}\right)^2\right]} \left[-K \; \text{Cos}\eta \; y^2 \frac{\partial \overline{\pi}}{\partial y} + \right.$$

$$\left. K \; \text{Sin} \; \eta \; y \frac{\partial \overline{\pi}}{\partial y} \right] = \frac{\partial^2 \overline{\pi}}{\partial y^2} \tag{3.13}$$

Define

$$\pi = \pi \; (\sigma) \tag{3.14}$$

and $\quad \sigma = y/\delta(\eta)$ $\hspace{4cm}$ (3.15)

where δ is the dimensionless local boundary layer thickness
[21]. Rewriting the equation (3.13) in terms of σ we
obtain:

$$\text{Re} \cdot \text{Sch} \cdot \sqrt{(1-(\tfrac{\sin\eta}{\cosh\beta_a})^2)} \; [-K \cos\eta \; \delta^3 - K \sin\eta \; \delta^2 \frac{\partial \delta}{\partial \eta}] \; \times$$

$$\sigma^2 \; \frac{d\pi}{d\sigma} = \frac{d^2\pi}{d\sigma^2} \hspace{3cm} (3.16)$$

Here we choose $\delta(\eta)$ such that

$$K \cos\eta \; \delta^3 + K \sin\eta \; \delta^2 \frac{\partial \delta}{\partial \eta} = \frac{3}{\text{Re} \cdot \text{Sch}\sqrt{(1-(\frac{\sin\eta}{\cosh\beta_a})^2)}}$$

$$\hspace{10cm} (3.17)$$

holds good, so that

$$\frac{d^2\pi}{d\sigma^2} + 3\sigma^2 \; \frac{d\pi}{d\sigma} = 0 \hspace{3cm} (3.18)$$

We have thus reduced the partial differential equation
(3.13) to an ODE (3.18). The boundary conditions for this
equation are:

$\quad$ (A) At $y=0$, $\pi=0$ $\quad$ (At spheroidal particle surface)

$\qquad$ or at $\sigma = 0$, $\pi=0$ $\hspace{4cm}$ (3.19)

$\quad$ (B) At $y = \beta_b - \beta_a \sim \infty$, $\quad \pi=1$ $\quad$ (at outer spheroidal

$\hspace{7cm}$ solid envelope)

or $\quad$ As $\sigma \rightarrow \infty$, $\quad \pi = 1$ $\hspace{3cm}$ (3.20)

Equation (3.18) can be integrated to obtain

$$\pi = K_1 \int_0^\sigma \text{Exp } (-t^3) \, dt + K_2$$

Where K_1 and K_2 are constants of integration and t
is a dummy variable. Application of the boundary conditions
yields the following concentration profile:

$$\pi = \frac{C_i - C_{io}}{C_{ico} - C_{io}} = \frac{1}{\Gamma(4/3)} \int_0^\sigma \exp(-t^3) dt \qquad (3.21)$$

The diffusional flux to any point on the surface of
the oblate spheroidal particle is

$$J = D_i \left(\frac{\partial C_i}{\partial \bar{Y}}\right)_{\bar{Y}=0} \qquad (3.22)$$

or

$$J = D_i \left(\frac{\partial C_i}{\partial y}\right)_{y=0} \left(\frac{\partial y}{\partial \bar{Y}}\right)_{\bar{Y}=0} \qquad (3.23)$$

Where $\bar{Y}$ is the distance from the surface along a
line of constant η and is a dimensional quantity, while y
is nondimensionalised $\bar{Y}$. The normal distance Y from any
point (β_a, η, φ) on an oblate spheroidal particle along
a line of constant η and φ to the corresponding point (β, η, φ) on
on a confocal oblate spheroidal surface is

$$\bar{Y} = C (\text{Sinh}\beta - \text{Sinh}\beta_a) \qquad (3.23)A$$

which can be reduced to the following by using (2.51) and
(2.55) for β being close to β_a

$$\bar{Y} = C \, \text{Cosh } \beta_a \, y \qquad (3.23B)$$

or

$$\left(\frac{\partial y}{\partial \bar{Y}}\right)_{\bar{Y}=0} = \frac{1}{C \, \text{Cosh}\beta_a} \qquad (3.24)$$

The differentiation of C_i with respect to y from equation (3.21) leads to

$$\frac{\partial C_i}{\partial y}\Big|_{y=0} = \frac{(C_i - C_{io})}{\Gamma(4/3)}\left(\frac{\partial \sigma}{\partial y}\right)_{y=0} = \frac{(C_{ico} - C_{io})}{\Gamma(4/3)} \frac{1}{\delta(\eta)} \quad (3.25)$$

The diffusional flux expression (3.23) may be reduced to the following by using (3.24) and (3.25):

$$J = \frac{D_i (C_{ico} - C_{io})}{C (4/3) \cosh\beta_a \, \delta(\eta)} \quad (3.26)$$

Substitution of the value of K from (3.12A) in (3.17) leads to the following partial differential equation for $\delta(\eta)$:

$$\delta^2 \sin\eta \frac{\partial \delta}{\partial \eta} + \cos\eta \cdot \delta^3 = \frac{3}{2} \times \frac{\cosh^2\beta_a}{\sinh\beta_a} \times \frac{G}{Re\ Sch}$$

or

$$\frac{\partial}{\partial \eta}(\delta^3 \sinh^3\eta) = \frac{9}{2} \times \frac{\cosh^2\beta_a}{\sinh\beta_a} \times \frac{G\ \sin^2\eta}{Re\ Sch}$$

After integrating it, one gets

$$\delta^3 \sin^3\eta = \frac{9}{2} \times \frac{\cosh^2\beta_a}{\sinh\beta_a} \times \frac{G}{Re\cdot Sch} \int_0^\eta \sin^2\eta\ d\eta$$

or

$$\delta^3 \sin^3\eta = \frac{9}{4} \times \frac{\cosh^2\beta_a}{\sinh\beta_a} \times \frac{G}{Re\ Sch} \left[\eta - \frac{\sin 2\eta}{2}\right] \quad (3.27)$$

The δ variation with η here is similar to that in Levich[21] for a sphere. At $\eta=\pi$, δ tends to infinity producing zero mass flux as in Levich [21]. This will only reduce the j value marginally.

Substitution of δ from (3.27) into the expression (3.26) reduces the diffusional flux expression to

$$J = \frac{D_i(C_{i\infty}-C_i)\,Sin\eta}{\Gamma(4/3)\cdot C\,Cosh\beta_a(\eta-\frac{Sin2\eta}{2})}^{1/3}\left[\frac{4}{9}\times\frac{Sinh\beta_a}{Cosh^2\beta_a}\times\frac{Re\cdot Sch}{G}\right]^{1/3}$$

$$(3.28)$$

The Sherwood number (based on the semi-major axis of the oblate spheroid) is a dimensionless estimate of the total diffusional flux to the surface of the oblate spheroidal particle. It can be estimated by integrating (3.28) over the particle surface as

$$Sh = \frac{C\,Cosh\,\beta_a\int J\,dS}{D_i(C_{i\infty}-C_i)\int dS} \qquad (3.29)$$

where

$$dS = \frac{d\eta\cdot d\varphi}{h_\eta\cdot h_\varphi}$$

or

$$dS = C^2 Cosh\,\beta_a\cdot Sin\eta\,\sqrt{(Cosh^2\beta_a-Sin^2\eta)}\,d\eta\cdot d\varphi$$

Thus

$$Sh = \frac{C\,Cosh\beta_a\int_0^{2\pi}\int_0^{\pi}J\,Sin\eta\,\sqrt{(Cosh^2\beta_a-Sin^2\eta)}\,d\eta\cdot d\varphi}{D_i(C_{i\infty}-C_i)\int_0^{2\pi}\int_c^{\pi}Sin\eta\,\sqrt{(Cosh^2\beta_a-Sin^2\eta)}\,d\eta\,d\varphi}$$

$$(3.30)$$

By substitution of the value of J from (3.28) into (3.30) and on simplification we get.

$$Sh = \left(\frac{4}{9}\right)^{1/3}\frac{1}{\Gamma(4/3)}\left[\frac{Re\cdot Sch}{G}\right]^{1/3}\cdot F(\beta_a) \qquad (3.31)$$

or $\quad Sh = 0.85423 \left[\dfrac{Re \cdot Sch}{G}\right]^{1/3} F(\beta_a)$ $\qquad\qquad$ (3.32)

where

$$F(\beta_a) = \dfrac{\displaystyle\int_0^\pi \dfrac{Sin^2\eta}{(\eta-\frac{Sin2\eta}{2})^{1/3}} \sqrt{(Cosh^2\beta_a - Sin^2\eta)} \quad d\eta}{Sinh^{2/3}\beta_a \ Cosh^{2/3}\beta_a \left[Coth\beta_a + \dfrac{Sinh\beta_a}{2} \ log_e\left(\dfrac{Cosh\beta_a+1}{Cosh\beta_a-1}\right)\right]}$$

$\qquad\qquad$ (3.33)

and G is defined by (2.32). The factor $F(\beta_a)$ has been
evaluated numerically using a computer program given in
Appendix D where the integral was evaluated by Trapezium
rule.

$\qquad$ Since it is preferable to define the Sherwood number
and Reynolds number with respect to the diameter for a
sphere, similarly the Sherwood and Reynolds numbers are now
defined with respect to the major axis of the oblate spheroidal
particle. Thus

$$Sh = \dfrac{0.85423 \times 2}{(2)^{1/3}} \left[\dfrac{Re \cdot Sch}{G}\right]^{1/3} F(\beta_a)$$

or $\quad Sh = 1.356 \left[\dfrac{U \cdot a}{D \cdot G}\right]^{1/3} F(\beta_a)$ $\qquad\qquad$ (3.34)

$\qquad$ Generally the Reynolds number in packed as well
as distended beds is defined with respect to the superficial
velocity U_s where

$$U_s = U \cdot \varepsilon \qquad\qquad (3.35)$$

where ε is the void volume fraction.

Further define $\quad Pe = \dfrac{U_s \cdot a}{D_i}$ $\hspace{3cm}$ (3.36)

By (3.34), (3.35) and (3.36) we get

$$Sh = 1.356 \left[\dfrac{Pe}{\varepsilon \ G} \right]^{1/3} F(\beta_a) \hspace{3cm} (3.37)$$

For a single oblate spheroidal particle in the flow field, the expression (3.37) reduces to the following

$$Sh = 1.356 \left(\dfrac{Pe}{G_\infty} \right)^{1/3} F(\beta_a) \hspace{3cm} (3.38)$$

where, as in relation (2.37), G_∞ is defined by

$$G_\infty = \text{Sinh } \beta_a - (\text{Sinh}^2 \beta_a - 1) \ \text{Cot}^{-1} \ \text{Sinh} \beta_a \hspace{2cm} (3.39)$$

Limiting Case: Single Sphere:

When $\beta_a \longrightarrow \infty$ $\quad$ (corresponding to $\dfrac{b}{a} \longrightarrow 1$) and $\varepsilon \longrightarrow 0$, $F(\beta_a)$ reduces to the following

$$F(\beta_a) = \dfrac{1}{2 \ \text{Sinh}^{1/3} \beta_a} \int_0^\pi \dfrac{\text{Sin}^2 \eta}{(\eta - \frac{\text{Sin} 2\eta}{2})^{1/3}} \ d\eta$$

$$F(\beta_a) = \dfrac{0.80515}{\text{Sinh}^{1/3} \beta_a} \hspace{3cm} (3.40)$$

(as shown in Appendix B)

and $\quad G = \dfrac{4}{3 \ \text{Sinh } \beta_a} \hspace{3cm} (3.41)$

(as shown in Appendix B)

By (3.40), and (3.41) the expression (3.37) for mass transfer to a single sphere in a fluid becomes

$$Sh = 1.356 \times 0.80515 \, (\tfrac{3}{4} \, Pe)^{1/3} \qquad (3.42A)$$

or

$$Sh = 0.992 \, (Pe)^{1/3} \qquad (3.42B)$$

which is Levich's classical solution for a single sphere[21].

The limiting solution for a cloud of spheres is difficult to obtain analytically. One may numerically determine the Sherwood number for an eccentricity value of $\frac{b}{a} = 0.99$ for obtaining results for a cloud of spheres.

3.2 Convective Diffusion to a Prolate Spheroidal Particle:

All the required expressions for a cloud of prolate spheroidal particles can be obtained from those for the oblate spheroidal cloud by simple transformations pointed out in Section 2.5.

For high Peclet and low Reynolds numbers, the Sherwood number (based on the major axis of the prolate spheroid) for a prolate spheroidal particle placed in a cloud of inactive identical prolate spheroidal particles is therefore given by

$$Sh = 1.356 \cdot [\frac{Pe}{\varepsilon \, G^*}]^{1/3} \, F^* \, (\beta_a) \qquad (3.43)$$

where

$$F^*(\beta_a) = \frac{\displaystyle\int_0^\pi \frac{\sin^2\eta}{(\eta - \frac{\sin^2\eta}{2})^{1/3}} \sqrt{(\sinh^2\beta_a + \sin^2\eta)} \, d\eta}{\cosh^{2/3}\beta_a \, \sinh^{2/3}\beta_a \, [\tanh\beta_a + \cosh\beta_a \, x}$$

$$\cot^{-1}\sinh\beta_a) \qquad (3.44)$$

and

$$G^* = \frac{\cosh\beta_b}{\sinh^2\beta_b} \sinh\beta_a + (1 + \cosh^2\beta_a) \, [\coth^{-1}\cosh\beta_a$$

$$-\coth^{-1}\cosh\beta_b] - \cosh\beta_a$$

$$(2.64.).$$

CHAPTER 4

RESULTS AND CONCLUSIONS FOR A CLOUD OF SPHEROIDAL PARTICLES

In this chapter, we will compare the results of the
present work on transport in a cloud of spheroidal particles
with other analytical or experimental results available
in literature. In the preceding chapter, an analytical
expression for estimating the diffusional flux to an active
spheroidal particle in a cloud of inactive spheroidal particles
was developed. The same expression may be used also for
predicting the diffusional flux to an active spheroidal
particle in a cloud of active spheroidal particles. Unfortu-
nately no work is available either in terms of hydrodynamics
around an oblate (or prolate) spheroidal particle in a cloud
of identical particles or in terms of the mass transfer rate
to or from the oblate (or prolate) spheroidal particle in a
cloud of identical particles (active or inactive). As the
present work covers a wide range of particle shapes lying
between the limits of thin circular disks and slender circular
cylinders without being valid for these two limiting cases
(see comments given later), one can compare existing results
for a spherical particle cloud with the results of the
present work when eccentricity of the spheroidal particles
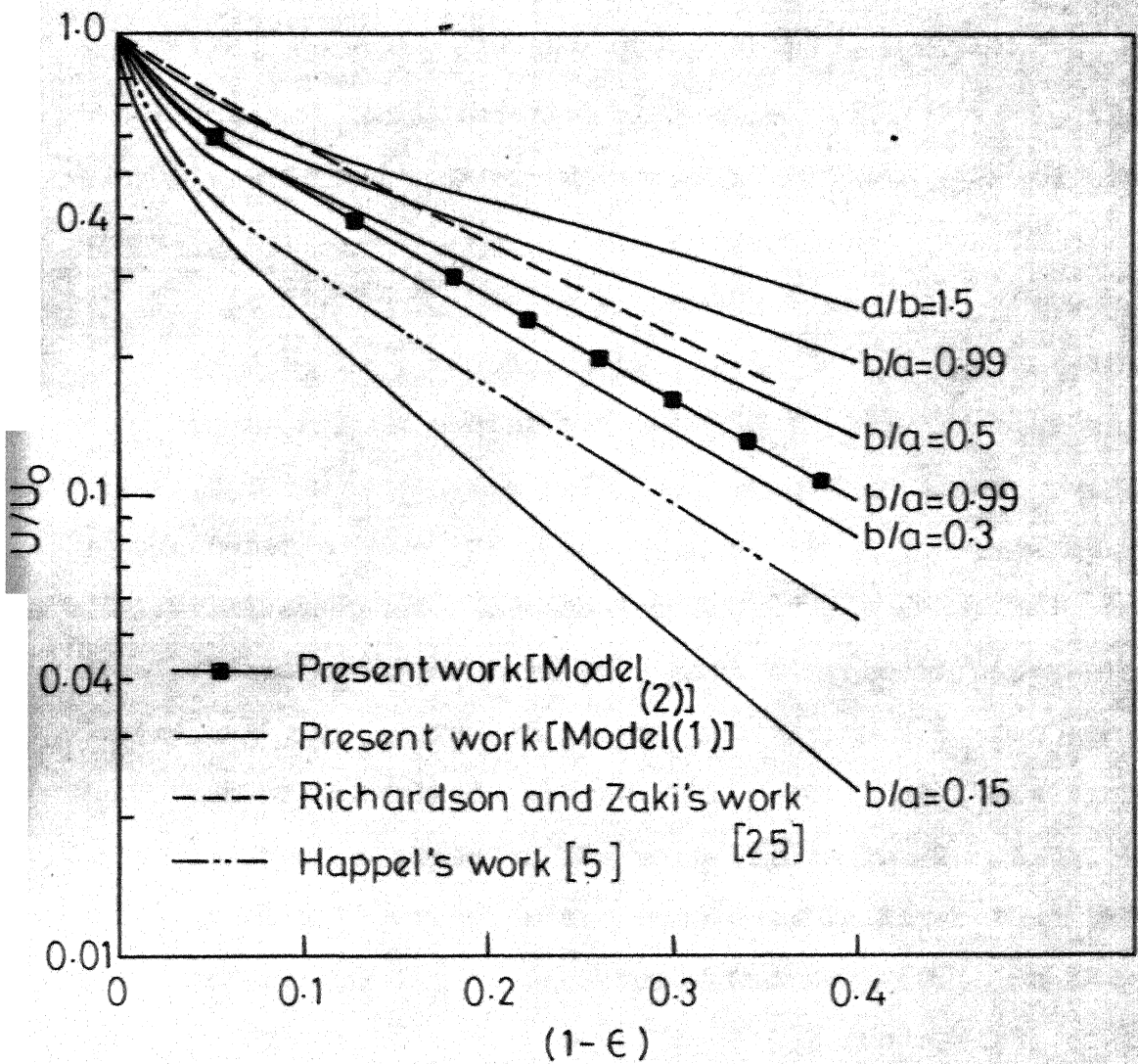tends towards unity, since a value of eccentricity of 0.99

Fig. 3 - Comparison of present work for U/U$_O$ with other experimental and analytical works (for sphere).

means that the spheroidal particles are almost of spherical shape. Great difficulty was encountered in obtaining an analytical solution for the particle shape of sphere when b=a because of some indeterminate terms and therefore the comparison is being carried out with spheroids of eccentricity b/a=0.99.

In Figure 3, the nondimensional ensemble average velocity U/U_o as per model 1 has been plotted against the void fraction ε according to equation (2.40) for various spheroidal shapes having different eccentricities. Happel [5] on the basis of the 'free surface' model has derived an analytical expression predicting U/U_o for a spherical particle cloud. Richardson and Zaki [25] have offered an expression on the basis of their experimental data for U/U_o for semimentation of Monosized spheres. The results of these two works have also been plotted on the same Figure 3. One notices that Happel's [5] results are considerably lower than the experimental results of Richardson and Zaki [25]. On the other hand, for an eccentricity equal to 0.99, the results of the present work as per model 1 are quite close to the experimental results of Richardson and Zaki [25] for both low as well as high particle concentrations, whereas model 2 results are much closer to those of Happel[5] as expected.

In Figure 4 the quantity normally used in mass transfer in packed beds and dispersions $Sh.Pe^{-1/3}$ has been plotted against the void fraction ε for various spheroidal shapes having different eccentricities. A considerable amount of work
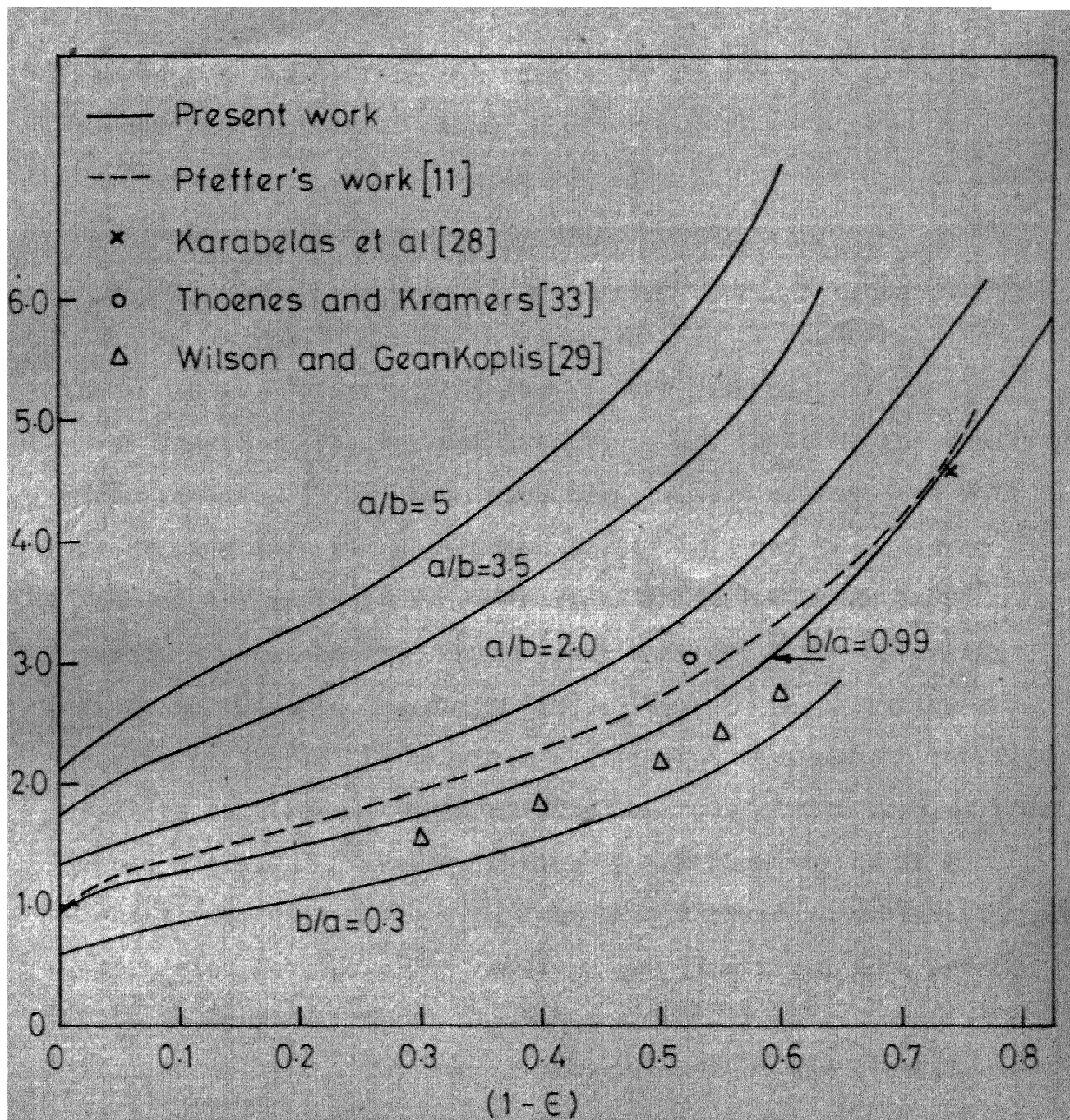
Fig. 4   -Comparison of present work for mass transfer with other experimental and analytical works (for sphere).

exists for the diffusional flux to or from a test particle placed in a spherical cloud of other spherical particles. Pfeffer [11], on the basis of Happel's [5] flow field around a sphere in an assemblage of spherical particles, obtained an analytical solution for the estimate of the total diffusional flux to or from a sphere in an assemblage of spherical particles. Pfeffer's [11] results are also plotted on the same Figure 4. For an eccentricity eq ual to 0.99, the results from equation (3.37) have also been plotted against the void fraction ε defined by equation (2.74). It may be observed that at all particle concentrations the curve of $Sh\ Pe^{-1/3}$ versus ε obtained from the present work for $(\frac{b}{a})= .99$ quite close to those of Pfeffer's [11]. solution. The solution of Sirkar [12] which is based on a different approach to the flow pattern in a random swarm of fixed spheres also resembles this curve of $Sh.Pe^{-1/3}$ versus ε closely for high values of ε. Recently Tardos et al. [26] (who have derived an analytical expression for $Sh.Pe^{-1/3}$ based on the flow field in a bed of uniform spheres proposed by Neale and Nader [27]) found a similar tendency. The recent measurements of the overall rate of mass transfer to a single sphere in a close packed cubic array of inert spheres ($\varepsilon = 0.26$) by Karabelas et al. [28] may also be compared with the results from the present derivation. Wilson and Geankoplis [29] on the basis of their experiments for a dilute bed of active and inactive spheres offered the following correlation:

$$Sh = \frac{1.09}{\varepsilon} Pe^{1/3} \qquad\qquad (4.1)$$

It is very clear from Figure 4 that a very good agreement exists between these experimental results and the results of the present work.

Thus the expressions derived in the present work predict scalar and vector transport satisfactorily when the spheroidal particle eccentricity (b/a) tends to unity corresponding to a cloud of spheroidal particles. One may therefore expect that the present solution will also predict reasonably well the scalar and vector transport for a particle cloud with particles having an eccentricity other than unity since the present solution predicts exactly the hydrodynamics of a single oblate (or prolate) spheroidal particle in the flow field. For example, it has been shown in Chapter 2, that the drag on a flat thin disk as well as that on an elongated rod. can be obtained from the present solutions for a single particle in the flow field. It may be possible to compute the Kozeny constant K for creeping flow through an assemblage of elongated rods with their axes parallel to the mean flow and compare these with those of other cell model solutions available in P-395 of Happel and Brenner [18].

For thecase of mass transfer, it is known, however, that there are no creeping flow solutions for Sherwood number for flow around a flat thin disk placed perpendicular to

flow [13]. No attempt has therefore been made to check the
validity of the existing solution for this limit. Further
the effect of the sharp discontinuity in flow directions at
the disk ends as well as the very tortuous paths of fluid
flow within an assemblage of disks at high concentrations are
not known at this time in so far as convective diffusion
analysis is concerned. Thus the limits of applicability of
the present solution are not available as the particle concen-
tration increases and the oblate spheroid tends to a disk.

CHAPTER 5

MASS TRANSFER IN A CLOUD OF DROPS AT HIGH SCHMIDT NUMBERS

A transfer of mass takes place between the dispersed
phase and the continuous phase in various chemical engineering
operations such as distillation, liquid liquid extraction,
spray drying etc where there exists direct contact between
the fluids. The study of mass transfer in such systems
requires the consideration of the effects of drop size distribution
presence of surfactant impurities, residence time distribution
etc. Padmanabhan and Gal-Or [24] and Yaron and Gal-Or [30]
had determined the total interfacial mass transfer rate in an
assemblage of drops dispersed in another liquid by probabili-
stically summing up the mass transport contributions of drops
in every size range. These two studies were based on the fluid
mechanics of an assemblage of round drops of uniform diameter
as carried out by Gal-Or and Waslo [17]. Recently Sirkar [19]
developed the velocity profile around a round test drop placed
in a size distributed cloud of round drops on the basis of
Tam's [6] solution for the flow field around a test sphere
placed in a size distributed cloud of spheres under conditions
of creeping flow. Therefore, the objective in this Chapter
is to derive an analytical result for the mass transfer
coefficient to a single active spherical drop inside a random
homogeneous isotropic cloud of inert spherical drops using
Sirkar's [19] velocity profile. This will enable us to check

the often used hypothesis 'Replace a size distributed system
of spherical particles or drops by a cloud of uniform sized
spherical particles or drops having the size equal to the
Sauter mean diameter of the size distributed system'. Here
we restrict ourselves to a cloud of round drops having a
uniform residence time. Further, high Peclet numbers and
low Reynolds numbers are assumed so that existing analytical
techniques are sufficient to obtain the required solution of
the convective diffusion equation. Lastly, a pure system
uncontaminated by surfactants is adopted for the sake of
simplicity.

5.1 Governing Equations for Mass Transport and Its Solution:

For viscous flow around a spherical particle or drop
(or bubble) of radius b, if the Schmidt number (ν/D_i) is
large and fluid is in creeping flow, a thin concentration
boundary layer is formed around the sphere or drop (or bubble)
from the front stagnation point. Since the Peclet number
($\frac{U_o 2b}{D_i}$) under such conditions is very large, the concentration
distribution for species i in the concentration boundary layer
may be described by the equation [21].

$$v_r \frac{\partial c_i}{\partial r} + \frac{v_\theta}{r} \frac{\partial c_i}{\partial \theta} = D_i \frac{\partial^2 c_i}{\partial r^2} \qquad (5.1)$$

At high Peclet numbers, the concentration change is
completed in a thin region very close to the interface of
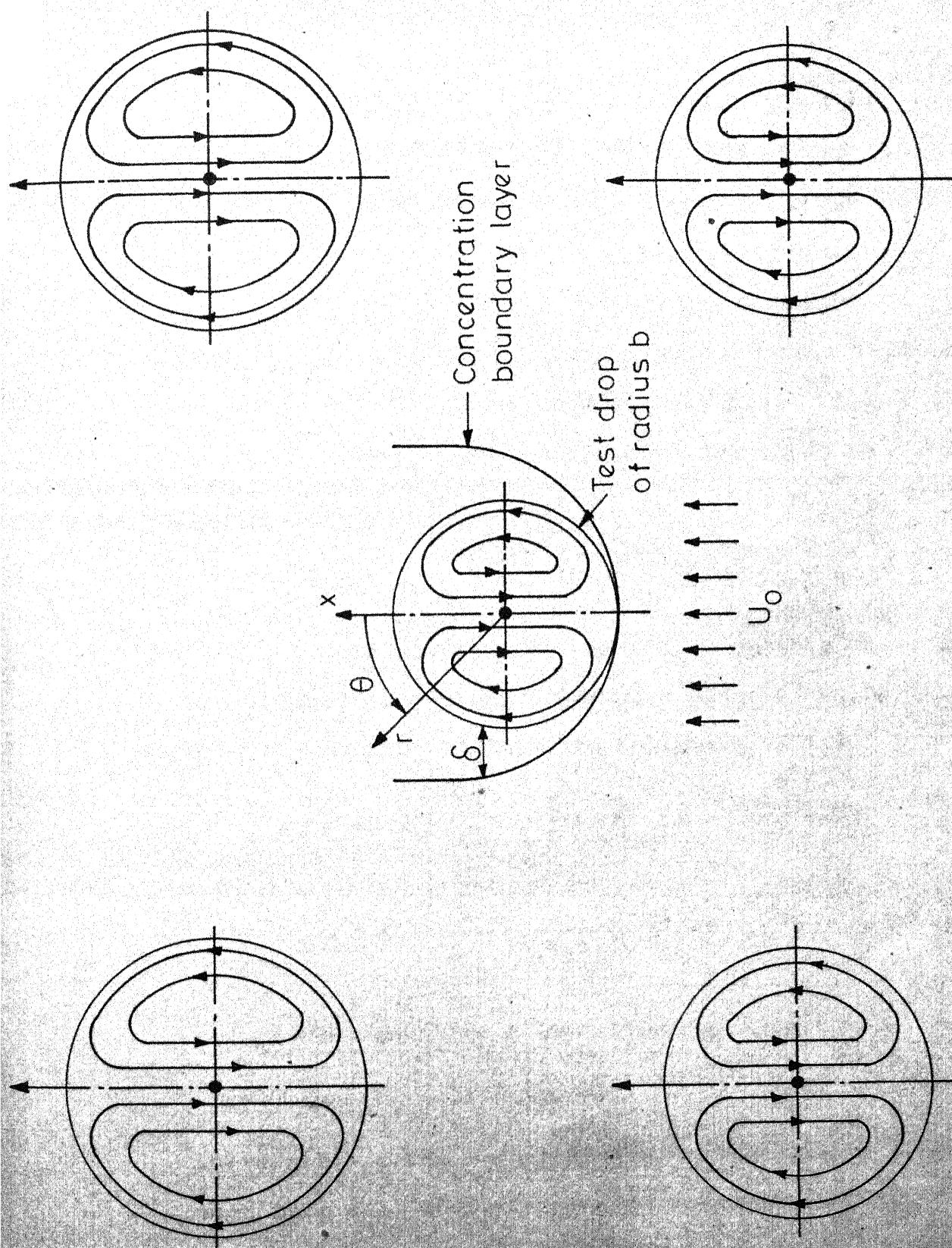the continuous fluid and the drop. This permits us to use the

Concentration boundary layer

Test drop of radius b

U_0

Fig. 5 - Coordinate system for creeping flow around the test drop in a cloud of drops.

velocity profile valid in this region. We assume that the thickness of the concentration boundary layer, δ, is very small compared to the radius of the active drop (or bubble), b. This is consistent with the high Peclet number assumption. Following Levich [21] (page 405) the variables (r, θ) of the spherical polar coordinate system are changed to (ψ, θ) where ψ is the stream function of the flow. Further an axisymmetric flow is assumed so that there is no $\emptyset$ dependence. The flow situation and coordinates are shown in Figure 5. The convective diffusion equation (5.1) then reduces to

$$(\frac{\partial c_i}{\partial \theta}) = D_i \; b^2 \; \sin^2\theta \; \frac{\partial}{\partial \psi} [b \; v_\theta \; \frac{\partial c_i}{\partial \psi}] \qquad (5.2)$$

For the continuous phase flow outside the round test drop placed in a size distributed cloud of round drops, Sirkar [19] had obtained the following velocity profile:

$$v_r = \cos\theta \; [U_o + \frac{2B}{r^3} + \frac{A}{a^2 r^3}(2 - 2e^{-ar} - 2ar \; e^{-ar})] \qquad (5.3)$$

and

$$v_\theta = [-U_o + \frac{B}{r^3} - \frac{A}{a^2 r^3} (e^{-ar} + ar \; e^{-ar} + a^2 r^2 e^{-ar} - 1)]$$
$$(5.4)$$

The quantity a is defined by (See Tam [6] or Sirkar[19])

$$\mu a^2 = n(b) \; D_r(b) \; db \qquad (5.5)$$

where $n(b)$ is the number density distribution of drop sizes such that $n(b)$ db is the number density of drops with radii between b and b+db and $D_r(b)$ is the coefficient depending on

the drop size b, the statistical properties of the cloud and the two fluid viscosities μ and $\bar{\mu}$ where $\bar{\mu}$ refers to the drop phase viscosity and μ to the continuous phase viscosity. To illustrate, the drag force in the jth direction on a drop of radius b on the basis of the point force approximation leads to

$$\text{Drag}\Big|_{\text{j dir}} = D_r(b) \; U_j \tag{5.5A}$$

where U_j is the unperturbed fluid velocity as seen by the drop in the jth direction at the centre of the particle of radius b in sense of Tam [6]. Sirkar [19] has determined the unknowns U_o, A and B in equation (5.4) in terms of the quantity 'a':

$$U_o = \frac{U_s}{W}[1 + f(1 + \frac{ab}{3})] \tag{5.6}$$

$$A = - U_s \left[\frac{b \, e^{ab} (3+2f)}{2W} \right] \tag{5.7}$$

and

$$B = U_s b \; \frac{(3+2f)(e^{ab}-1-ab) - a^2 b^2[1+f(1+\frac{ab}{3})]}{2 \, a^2 W} \tag{5.8}$$

where

$$U_s = \frac{2(\bar{\rho} - \rho) \, g \, b^2}{g \, \mu} \tag{5.9}$$

$$W = [1+ab+ \frac{a^2 b^2}{3} + \frac{2f}{3} (1+ab + \frac{a^2 b^2}{2} + \frac{a^3 b^3}{6})] \tag{5.10}$$

and $\quad f = \mu/\bar{\mu} \tag{5.11}$

The quantity ab has to be obtained from a solution of the following equation

$$a^2 = 6\pi \int_0^\infty b n(b) \left[\frac{1+ab+ \frac{a^2 b^2}{3} + f(\frac{2}{3} + \frac{2ab}{3} + \frac{a^2 b^2}{3} + \frac{a^3 b^3}{9})}{1 + f(1+ \frac{ab}{3})} \right] \times db \tag{5.11a}$$

Since $D_r(b)$ is given by

$$D_r(b) = \frac{6\pi b\mu \left[1+ab+ \frac{a^2 b^2}{3} + f(\frac{2}{3} + \frac{2ab}{3} + \frac{a^2 b^2}{3} + \frac{a^3 b^3}{9})\right]}{1 + f(1+ \frac{ab}{3})} \tag{5.11b}$$

The stream function for the continuous phase around the round test drop was also determined by Sirkar [19] to be

$$\psi = - \frac{U_o r^2 \sin\theta}{2} - \frac{B \sin^2\theta}{r} + \frac{A \sin^2\theta}{a^2 r} [e^{-ar}(1+ar)-1] \tag{5.12}$$

Substituting $r=(b+y)$ in the expression (5.12) for the radial coordinate of any point in the concentration boundary layer and expanding it in terms of powers of y leads to

$$\psi = - \frac{U_o (1+ab) \sin^2\theta}{4[1+f(1+ \frac{ab}{3})]} \times [2bfy + (3+2f) y^2]$$

$$+ \text{ Terms with higher powers} + \ldots\ldots \atop \text{of } y \tag{5.13}$$

The terms containing y^3 and higher powers of y may be neglected as the Peclet number is assumed to be very high and we are concerned with very small values of y close to the drop surface. Thus

$$\psi \cong - \frac{U_o(1+ab) \sin^2\theta}{4[1+f(1+ \frac{ab}{3})]} \times [2bfy + (3+2f)y^2] \tag{5.14}$$

and

$$b \, v_\theta = \frac{b}{r \sin\theta} \frac{\partial \psi}{\partial r}$$

$$\cong - \frac{1}{\sin\theta} \times \frac{U_o(1+ab)\ \sin^2\theta}{4[1+f(1+\frac{ab}{3})]} \times [2bf + 2(3+2f)y] \tag{5.15}$$

Substitution of y in terms of   from (5.14) in (5.15) leads to

$$bv_\theta = - \sqrt{[\frac{U_o(1+ab)\ (3+2f)}{1+f\ (1+\frac{ab}{3})}]} \ \sqrt{(z-\psi)} \tag{5.16}$$

where

$$Z = \frac{b^2 f\ U_o(1+ab)\ \sin^2\theta}{4(3+2f)\ [1+f(1+\frac{ab}{3})]} \tag{5.17}$$

Substituting $b\,v_\theta$ from (5.16) into the simplified convective diffusion equation (5.2) leads to

$$\frac{\partial c_i}{\partial \theta} = - D_i\ b^2\ \sin^2\theta\ \sqrt{[\frac{U_o(1+ab)\ (3+2f)}{1 + f(1+\frac{ab}{3})}]} \ . \ x$$

$$\frac{\partial}{\partial \psi}[\sqrt{(z-\psi)} \ \frac{\partial c_i}{\partial \psi}] \tag{5.18}$$

A completely general analytical solution for this type of P.D.E. is difficult as has been pointed out by Gal-Or and Waslo[17]. For the limiting case of solid particles or for fluid dispersed phase with very little internal circulation (i.e. $f \Rightarrow 0$), equation(5.18) becomes

$$\frac{\partial c_i}{\partial \theta} = -D_i\ b^2\ \sin^2\theta\ \sqrt{[3U_o(1+ab)]} \frac{\partial}{\partial \psi}[\sqrt{-\psi} \frac{\partial c_i}{\partial \psi}] \tag{5.18A}$$

This equation is identical to that used by Sirkar [12] for obtaining the dimensionless diffusional flux to a single

active spherical particle in a random spherical inactive particle cloud at high Schmidt numbers.

For the other limiting case of rapid circulation inside the drops, the quantity f has a very large value so that $Z \gg \psi$ and equation (5.18) reduces to

$$\frac{\partial c_i}{\partial \theta} = - \frac{D_i U_o f b^3 \sin^3\theta (1+ab)}{2[1 + f(1 + \frac{ab}{3})]} \frac{\partial^2 c_i}{\partial \psi^2} \qquad (5.19)$$

Define $\theta' = \pi - \theta$ because the concentration boundary layer starts growing from $\theta = \pi$ towards $\theta = 0$ (See Fig.5) in a direction opposite to that of the positive θ coordinate. Using equation (5.6) and changing the θ variable to θ' leads to

$$\frac{\partial c_i}{\partial \theta'} = \frac{D_i U_s f (1+ab) b^3 \sin^3\theta'}{2W} \frac{\partial^2 c_i}{\partial \psi^2} \qquad (5.20)$$

The boundary conditions are

(a) $c_i = 0$, at $\psi = 0$ (at the interface) (5.21)

(b) $c_i = c_{i0}$ at $\psi = 0$ (front stagnation point)
      and $\theta' = 0$ (5.22)

(c) $c_i = c_{i0}$ as $\psi \to -\infty$ (far from the drop) (5.23)
(corresponding to the concentration in the incoming fluid)

For the same boundary conditions, Levich [21] has solved a partial differential equation very similar to the equation (5.20). If in equation (5.20) the quantity $\frac{U_s f (1+ab)}{2W}$, is replaced by U_s, the total diffusional flux to the drop interface, I_b, was obtained by Levich [21] to be

$$I_b = 8 \; C_{io} \; \sqrt{\left(\frac{\pi}{3}\right)} \left[\frac{D_i \; U_s}{b}\right]^{\frac{1}{2}} \; b^2 \tag{5.24}$$

In the present case, therefore, the total diffusional flux to the interface of the test drop can be easily shown to be

$$I_b = 8 \; C_{io} \sqrt{\left(\frac{\pi}{3}\right)} \left[\frac{D_i \; U_s (1+ab) \; f}{2 \; W \; b}\right]^{\frac{1}{2}} \; b^2 \tag{5.25}$$

The Sherwood number may be considered as the dimensionless diffusional flux to the total interface of the drop. Therefore the Sherwood number defined with respect to the diameter of the drop is obtained from (5.25) as

$$Sh = \frac{2I_b \cdot b}{4\pi b^2 \; D_i \; C_{i\infty}}$$

or

$$Sh = \frac{2}{\sqrt{(3\pi)}} \left[\frac{f \; (1+ab)}{W} \; x \; \frac{2U_s \cdot b}{D_i}\right]^{\frac{1}{2}}$$

or

$$Sh = \frac{2}{\sqrt{(3\pi)}} \left[\frac{f(1+ab)}{W} \; x \; \frac{2 \; U_s \; b}{D} \; x \; Sch\right]^{\frac{1}{2}} \tag{5.26}$$

Using (5.6), we get

$$Sh = \frac{2}{\sqrt{(3\pi)}} \left[\frac{f(1+ab)}{1+f \left(1+ \frac{ab}{3}\right)} \; x \; \left(\frac{2 \; U_o \; b}{D}\right) \; x \; Sch\right]^{\frac{1}{2}} \tag{5.26A}$$

For a single drop (or bubble) in an infinite fluid (i.e. drop concentration, $C \rightarrow 0$ and $ab \rightarrow 0$), the equation (5.26A) reduces to

$$Sh = 0.653 \left[\frac{\mu}{\overline{\mu} + \mu}\right]^{\frac{1}{2}} Re^{\frac{1}{2}} \; Sch^{\frac{1}{2}} \tag{5.26B}$$

which is identical to Levich's [21] solution.

5.2 Interpretation of Mass Transfer Coefficients in a Cloud of Drops (or Bubbles):

In the preceding section 5.1, the mass transfer coefficient for mass transfer to or from an active drop (or bubble) moving in the continuous phase has been obtained when all other drops (or bubble) are inactive. When all other drops are active, the effect of concentration wakes from previous drops will affect the boundary conditions for the present problem. It is not known how one could solve the problem exactly for such a situation in a cloud of drops. The existing approaches are similar to that of Gal-Or and Hoelscher [15]. These authors had evaluated the total rate of mass transfer $\bar{N}_T$ in the whole vessel, by carrying out an integration over the entire surface of the swarm of drops in the following manner:

$$\bar{N}_T = \int_O^A \bar{N}_A \, dA \qquad (5.27)$$

where $\bar{N}_A$ is the average diffusional flux to the surface of a single drop of size b such that dA is the total surface area of drops in the size range of b to b+db. These drops constitute a subreactor as proposed by Gal-Or and Resnick [31]. For example, for spherical drops in the size range of b to b+db, $dA = \dfrac{3 \, V_T}{b} \, dC$ where C is the dispersed phase volume fraction and V_T is the total volume of the vessel. Gal-Or and Hoelscher [15] had related the total interfacial area A between the dispersed and the continuous phases, with a suitable size

distribution function n(b) for drops (or bubbles), void
fraction and the average drop (or bubble) radius. By such
an analysis, they had evaluated the average mass transfer
coefficient $\bar{N}_T$ for the continuous phase with size distribution
and compared this average mass transfer coefficient with the
average mass transfer coefficient evaluated on the basis of
a uniform size of the droplets in the cloud when each drop
(or bubble) is replaced by a drop (or bubble) having a size
equal to the volume surface mean radius $\bar{b}_{32}$ of the dispersion
defined by

$$\bar{b}_{32} = \frac{\int_0^\infty b^3 \, n(b) \, db}{\int_0^\infty b^2 \, n(b) \, db} \tag{5.27b}$$

A similar approach is being adopted herewith regard
to the mass transfer coefficient derived in the preceding
section on the basis of Sirkar's [19] velocity profile. However,
the difference between the two analyses are: Gal-Or and
Hoelscher [15] used Levich's [21] equation for mass transfer
coefficient obtained for a single drop in the flow field where-
as the mass transport analysis in our case is based on the
velocity profile through a cloud of size distributed drops.
The assumption that all the drops (or bubbles) are exposed to
the same interfacial as well as bulk concentration leads to
the following expression for the total mass transfer rate from
the continuous phase to the interface per unit volume of the
contactor vessel:

$$\bar{N}_T = \int_o^\infty I_b \, n(b) \, db \qquad (5.28)$$

where $n(b)$ is the drop (or bubble) size distribution function such that $n(b)db$ is the number density of drops (or bubbles) with radius lying between b and $(b+db)$. Substitution of I_b from (5.25) into (5.28) leads to

$$\bar{N}_T = \text{\& } C_{io} \sqrt{(\tfrac{\pi}{6} D_i f)} \int_o^\infty [\frac{U_s (1+ab) \; b^3}{W}]^{\frac{1}{2}} n(b) \, db \qquad (5.29)$$

The total interfacial area per unit volume between the dispersed phase and the continuous phase, A_T, is, then

$$A_T = \int_o^\infty 4\pi \, b^2 \, n(b) \, db \qquad (5.30)$$

The overall average mass transfer coefficient for the size distributed bubbles (or drops) may be defined as

$$\bar{K}_{SD} = \frac{\bar{N}_T}{C_{io} \, A_T} \qquad (5.31)$$

Using (5.29) and (5.30) leads to

$$\bar{K}_{SD} = \sqrt{(\frac{2D f}{3\pi})} \; \frac{\int_o^\infty [\frac{U_s (1+ab) \; b^3}{W}]^{\frac{1}{2}} n(b) \, db}{\int_o^\infty b^2 \, n(b) \, db} \qquad (5.32)$$

Substituting U_s from (5.9) into (5.32) leads to

$$\bar{K}_{SD} = \sqrt{\frac{4 D f \; (\bar{\rho}' - \rho) g}{27 \, \pi \, \mu}} \; \frac{\int_o^\infty [\frac{(1+ab) \; b^5}{W}]^{\frac{1}{2}} n(b) \, db}{\int_o^\infty b^2 \, n(b) \, db}$$

or

$$\bar{K}_{SD} = \bar{R}_{SD} \; \sqrt{(\frac{4 \; Df(\bar{\rho}' - \rho) \; g}{27 \; \pi \; \mu})} \tag{5.33}$$

where

$$\bar{R}_{SD} = \frac{\displaystyle\int_0^{co} \sqrt{(\frac{(1+ab)}{W})b^5)} \; n(b) \cdot db}{\displaystyle\int_0^{co} b^2 \; n(b) \; db} \tag{5.34}$$

Here the factor ab for a particular drop size b is a function of the dispersed phase concentration c the viscosity ratio f and the size distribution function $(n(b)/N)$ as given in equations (5.11 a,b).

However, if we replace the size distributed system by a system of uniform drops (or bubbles) of size $\bar{b}_{32}$, derived from the same size distributed system, the value of 'a' will change to '$\bar{a}$'. Therefore the average mass transfer coefficient in the Gal-Or and Hoelscher [15] sense with such a hypothetical cloud will be

$$\bar{K}_{UD} = \frac{I_b(\bar{b}_{32})}{c_{io} \; 4\pi \; \bar{b}_{32}^2} \tag{5.35}$$

Substituting for I_b with $b = \bar{b}_{32}$ from (5.25) into (5.35) and using (5.9) leads to

$$\bar{K}_{UD} = \bar{R}_{UD} \; \sqrt{(\frac{4 \; Df(\; ' - \;) \; g}{27 \; \pi \; \mu})} \tag{5.36}$$

$$\bar{R}_{UD} = \sqrt{\left[\frac{(1+\bar{a}\bar{b}_{32})\ \tilde{b}_{32}}{W\ (\bar{a}\ \bar{b}_{32})} \right]} \tag{5.37}$$

The quantity 'a' in equation (5.34) is defined by equation (5.11a) and (5.11b) for a particular size distribution function $n(b)/N$. We can assume, for example, that the drop size distribution $n(b)/N$ may be approximated by that proposed by Bayens [32] for coagulation of hydrosols and subsequently modified by Gal-Or and Hoelscher [15]:

$$\frac{n(b)}{N} = f(b)\ 4\ \left[\frac{\alpha_o^3}{\pi} \right]^{\frac{1}{2}} b^2\ \exp\ [-\alpha_o b^2] \tag{5.38}$$

where

$$\alpha_o = \left[\frac{4}{\sqrt{\pi}\ (\bar{b}_3)^3} \right]^{2/3} \tag{5.39}$$

and

$$\bar{b}_3 = \left[\int_0^\infty b^3\ f(b)\ db \right]^{1/3} \tag{5.40}$$

The quantity N which is the total number of drops (or bubbles) per unit volume may be related to the volume concentration, C, of drops by

$$N = \frac{C}{\frac{4}{3}\pi\ \bar{b}_3^{\ 3}} \tag{5.41}$$

where $\bar{b}_3$ is the volume mean radius defined by (5.40).

Substitution of N from (5.41) into (5.38) leads to

$$n(b) = \frac{3C}{\bar{b}_3^3}\ \left(\frac{\alpha_o}{\pi} \right)^{3/2} b^2\ \exp\ [-\alpha_o\ b^2] \tag{5.42}$$

For a size distributed cloud of drops (or bubble), the required value of 'a' may be obtained from (5.11a) and (5.11b) for the number density distribution function defined by (5.42). The integration limits of distribution function are preferably the maximum and minimum drop (or bubble) size in any distribution. For the distribution function (5.42), the cumulative percent volume of drops (or bubbles) with $\frac{\bar{b}_3}{10} \leqslant b \leqslant 5\bar{b}_3$ covers the range 0.062 per cent to 99.963 per cent. Thus one can use these integration limits without any significant error.

The factor $\bar{a}\,\bar{b}_{32}$ in equation (5.37) can be obtained from equation (5.11a) and reduces to the following as given by Sirkar [19] for a uniform size droplet cloud:

$$\bar{a}^3\bar{b}^3_{32}\left[\tfrac{f}{3}(1- \tfrac{3C}{2})\right] + \bar{a}^2\bar{b}^2_{32}\left[1 + f\left(1 - \tfrac{3C}{2}\right)\right]$$

$$-\bar{a}\,\bar{b}_{32}\left[(6+4f)\,\tfrac{3C}{4}\right] - \tfrac{3C}{4}(6 + 4f) = 0 \qquad (5.43)$$

If one knows the viscosity ratio of two fluids and the volume concentration of drops, the factor $\bar{a}\,\bar{b}_{32}$ for a cloud of uniform radius $\bar{b}_{32}$ can be obtained from this cubic equation (5.43).

After obtaining the value of 'a' and '$\bar{a}$', it is possible to find the coefficient $\bar{R}_{SD}$ in equation (5.33) and $\bar{R}_{UD}$ in equation (5.36) for different sets of values of f, the viscosity ratio of two fluids, C, the volume concentration of drops (or bubbles) and given values of $\bar{b}_{32}$. Thus, with regard

to mass transfer in creeping flow one may compare $\bar{R}_{SD}$ and $\bar{R}_{UD}$ to check the often used hypothesis 'Replace a size distributed system of spherical particles or drops by a cloud of uniform sized spherical particles or drops having the size equal to the Sauter mean diameter of the size distributed system'.

Another way to look at the effect of the size distribution is to consider the mass transfer coefficient to an active drop of size b inside a cloud of inactive drops.

The cloud of inactive drops may be considered to be either size distributed or having a uniform size equal to $\bar{b}_{32}$ of the size distributed system.

The average mass transfer coefficient, K_{SD}, for an active drop of radius b, placed in a inactive size distributed cloud is obtained from equation (5.25) as

$$K_{SD} = \frac{I_b}{C_{iO}\, 4\pi\, b^2}$$

or

$$K_{SD} = R_{SD}\ \sqrt{\left[\frac{4}{27}\ \frac{f \cdot b\ (\bar{\rho}' - \rho)\ g}{\pi\ \mu}\right]} \qquad (5.44)$$

where

$$R_{SD} = \sqrt{\left[\frac{(1 + ab)}{W(ab)}\right]} \qquad (5.45)$$

Similarly, one can also define the average mass transfer coefficient, K_{UD}, for an active drop of radius b, placed in an inactive cloud of drops of uniform size equal

to $\bar{b}_{32}$ of the size distributed system:

$$K_{UD} = \frac{I_b}{c_{i0} \; 4\pi \, b^2}$$

or

$$K_{UD} = R_{UD} \; \sqrt{\left[\frac{4}{27} \times \frac{fb(\rho'-\rho)\,g}{\pi \, \mu}\right]} \tag{5.46}$$

where

$$R_{UD} = \sqrt{\left[\frac{1 + \bar{a}\,\bar{b}_{32}\,(\frac{b}{b_{32}})}{W(\overline{ab}_{32}\frac{b}{b_{32}})} b_{32}\right]} \tag{5.47}$$

The factors 'ab' and '$\bar{a}\,\bar{b}_{32}$' in equations (5.45) and (5.47) respectively may be determined exactly in the same way it was determined earlier in this section. Thus one can compare the value of R_{SD} and R_{UD} for different sets of f, C and different values of b and can determine whether a size distributed cloud may be replaced by an uniform sized cloud for mass transfer in creeping flow.

A recent experimental work by Tan et. al.[20] on the mass transfer coefficient in a packed bed of active spheres involved three different diameters of benzoic acid spheres. Such a discontinuous distribution described in Table 1 of Tan et al.[32] may be represented by

$$n(b) = \frac{3c}{4\pi \, b_3^3}[x_{0.51}\delta(b-0.51)+x_{0.71}\delta(b-0.71)+x_{1.15}\delta(b-1.15)] \tag{5.48}$$

where $x_{0.51}$ is the fraction of spheres having the radius 0.51 cm in the mixture which had spheres of two other radii, 0.71 cm and 1.15 cm, and $\delta(b-0.51)$ is Dirac delta function with a value of unity when b=0.51 and 0 when b≠0.51. The relative fraction of spheres of each size are available in Tan et al.[32]. Such a distribution function will be useful for comparing the predicted effect of size distribution with that observed experimentally by Tan et al.[32] in the other limit of a cloud of solids particles, or almost solid-like drops.

CHAPTER 6

RESULTS AND CONCLUSIONS FOR A CLOUD OF
SIZE DISTRIBUTED DROPS (OR BUBBLES)

The expression (5.26) derived in the preceding
chapter should be compared with the existing work on the value
of the Sherwood number for a single active drop (or bubble)
inside a random cloud of inactive drops (or bubbles) for high
Schmidt numbers and low Reynolds numbers. Unfortunately very
little work is available for a size distributed cloud of
drops (or bubbles), in the literature under conditions of no
surfactant contamination.

Gal-Or and Waslo [17] had made the analysis for the
present problem but on the basis of a uniform size of droplets
in the cloud. The value of the quantity $Sh\ Pe^{-1/2}$ calculated
from expression (5.26A) for different void volume fractions
on the basis of uniform size has been compared with the same
quantity $Sh\ Pe^{-1/2}$ calculated from Gal-Or and Waslo's [17]
work, for two different ratios of viscosity of continuous
phase and viscosity of dispersed phase. It is obvious from
Table 1 that the estimate of the quantity $Sh\ Pe^{-1/2}$ from
the present work is somewhat less than the value of the
similar quantity from the expression given in Gal-Or and
Waslo [17] based on the 'free surface cell' model, *especially*
at high volume concentrations of drops (or bubbles) where

TABLE I: COMPARISON OF PRESENT MODEL WITH WASLO
AND GAL-OR'S MODEL FOR A CLOUD OF DROPS
OF UNIFORM SIZE

Volume concen-tration of dispersed phase, C	$Sh\ Pe^{-1/2}$			
	f=10		f=100	
	Present work	Waslo-Gal-Or [17]	Present work	Waslo-Gal-Or [17]
0.00	0.6225	0.6225	0.6497	0.6497
0.05	0.7069	0.7932	0.7337	0.8181
0.10	0.7373	0.8654	0.7635	0.8888
0.15	0.7634	0.9288	0.7890	0.9507
0.20	0.7900	0.9898	0.8156	1.0100
0.30	0.8415	1.1149	0.8554	1.1300
0.40	0.8850	1.2540	0.8946	1.2700
0.50	0.9284	1.4217	0.9405	1.4363
0.60	0.9969	1.6366	1.0040	1.6488

in the limit of the dispersed phase hold up fraction approaching 2/3, the present solution breaks down. The non-applicability of the present work for high value of dispersed phase holdup fraction follows from the point force approximation and the assumption of no drop-drop (or bubble-bubble) correlation in Sirkar's [19] derivation of velocity profile through the cloud of size distributed drops (or bubbles). It is appropriate at this stage to notice that Sirkar [12] found a similar tendency when he compared his results for creeping flow mass transfer to a single active sphere in a random spherical particle cloud with those from the work of Pfeffer [11].

The expressions (5.33) and (5.36) of the preceding chapter predict the overall mass transfer coefficient for the size distributed active cloud of bubbles (or drops) and for the active cloud of bubbles (or drops) of uniform size $\bar{b}_{32}/b_{32}$ respectively. The expressions (5.44) and (5.46) predict the mass transfer coefficient for the active test bubble (or drop) placed in an inactive cloud of size distributed bubbles (or drops) and the mass transfer coefficient for the active test bubble (or drop) placed in an inactive cloud of bubbles (or drops) of uniform size $\bar{b}_{32}$. Here $\bar{b}_{32}$ the Sauter mean radius of the size distributed suspension. Thus the predictions for a size distributed cloud should be compared with the predictions for a cloud of uniform size, $\bar{b}_{32}$, so that one can find the magnitude of possible error if the size-distributed

cloud is replaced by a uniform sized cloud having the same Sauter mean radius.

Using the size distribution function (5.38) of Gal-Or and Hoelscher [15], calculations have been carried out on computer (IBM 1401, see Appendix D) for a cloud of drops (or bubbles) for three different values of viscosity ratio, f. All the calculations are based on the mean volume radius $\bar{b}_3=0.01$ cm. Here it should be pointed out that one can also carry out the calculations based on some different value of the mean volume radius $\bar{b}_3$, but the conclusions will not differ as was found out. These results are shown in Tables, II, and III where the magnitudes of $\bar{R}_{SD}$, $\bar{R}_{UD}$, R_{SD}, R_{UD} are reported for various cases. In Table II, the factors $\bar{R}_{SD}$ and $\bar{R}_{UD}$ in expressions (5.35) and (5.36), respectively, have been compared for different viscosity ratios and for different dispersed phase volume concentrations. It is obvious from this table that in no case the possible error is more than 6 per cent when one replaces the size distributed cloud of active bubbles (or drops) by a uniform sized cloud of active bubbles (or drops) by a uniform sized cloud of active bubbles (or drops) having the same Sauter mean radius $\bar{b}_{32}$. Table III is concerned with an active bubble (**or drop**) of size, b, placed in a cloud of inactive bubbles (or drops) having the volume surface mean radius $\bar{b}_{32}$. The factors R_{SD} and R_{UD} in expressions (5.44) and (5.46), respectively, are reported in Table III. Here it should be pointed out that the results will be different as the normalized size $(b/\bar{b}_{32})$ of the active drop will vary.

TABLE II: COMPARISON OF $\bar{R}_{SD}$ AND $\bar{R}_{UD}$ FOR AN ACTIVE CLOUD OF DROPS (OR BUBBLES)

Volume Concentration of dispersed phase, C	f=0.1			f = 10.0			f = 100.0		
	$\bar{R}_{SD}$	$\bar{R}_{UD}$	Expected % error in $\bar{R}_{UD}$	$\bar{R}_{SD}$	$\bar{R}_{UD}$	Expected % error in $\bar{R}_{UD}$	$\bar{R}_{SD}$	$\bar{R}_{UD}$	Expected % error in $\bar{R}_{UD}$
0.05	0.09790	0.09983	1.965	0.03640	0.03724	2.317	0.01225	0.01251	2.126
0.15	0.08893	0.09169	3.114	0.03293	0.03402	3.321	0.01108	0.01149	3.744
0.25	0.07959	0.08222	3.302	0.02935	0.03057	4.147	0.00987	0.01027	4.084
0.35	0.06929	0.07166	3.424	0.02549	0.02681	5.165	0.00857	0.00895	4.393
0.45	0.05722	0.05925	3.534	0.02109	0.02207	4.673	0.00709	0.00745	5.014
0.55	0.04169	0.04346	4.253	0.01558	0.01623	4.148	0.00524	0.00547	4.323

TABLE III: COMPARISON OF R_{SD} AND R_{UD} FOR AN INACTIVE CLOUD (FOR f=0.1)

f	Viscosity ratio	Volume concentration of dispersed phase, C	$\dfrac{b}{b_{32}} = 0.1$			$\dfrac{b}{b_{32}} = 2.7$			$\dfrac{b}{b_{32}} = 10.8$		
			R_{SD}	R_{UD}	Expected % error in R_{UD}	R_{SD}	R_{UD}	Expected % error in R_{UD}	R_{SD}	R_{UD}	Expected % error in R_{UD}
0.1	0.1	0.1	0.9841	0.9814	0.004	0.7721	0.7766	0.581	0.4088	0.4128	0.981
		0.2	0.9631	0.9634	0.027	0.5879	0.5951	1.210	0.2800	0.2855	1.950
		0.4	0.9426	0.9442	0.176	0.3704	0.3792	2.380	0.1417	0.1465	3.320
	10.0	0.1	0.3621	0.36213	0.008	0.2614	0.2665	1.970	0.0912	0.0944	3.540
		0.2	0.3599	0.36000	0.0326	0.1913	0.1974	3.180	0.0636	0.0666	4.710
		0.4	0.3561	0.3566	0.1222	0.1121	0.1167	4.120	0.0320	0.0336	4.880
	100.0	0.1	0.1234	0.12342	0.011	0.0851	0.0868	2.100	0.0298	0.0312	4.720
		0.2	0.1211	0.1212	0.036	0.0639	0.0662	3.700	0.0209	0.0221	5.450
		0.4	0.1199	0.1200	0.1117	0.0374	0.0389	3.910	0.0106	0.0111	4.590

TABLE IV: MASS TRANSFER COEFFICIENT IN A SHALLOW PACKED BED OF ACTIVE SPHERES SIZE DISTRIBUTED AS PER TAN et al. [32]

Void Volume Fraction ε	Re=2.0 Calculated values of $(Sh)(Sc)^{-1/3}$ for different Mixtures of active spheres [32]				Observed value of $(Sh)(Sc)^{-1/3}$ [32]	Re=10.0 Calculated values of $(Sh)(Sc)^{-1/3}$ for different mixtures of active spheres [32]				Observed value $(Sh)(Sc)^{-1/3}$ [32]
	Mix.1	Mix.2	Mix.3	Mix.4		Mix.1	Mix.2	Mix.3	Mix.4	
0.70	2.267	2.269	2.254	2.270	2.00	3.876	3.881	3.854	3.882	3.65
0.65	2.456	2.465	2.446	2.446	2.16	4.201	4.200	4.185	4.217	3.93
0.60	2.673	2.668	2.669	2.693	2.32	4.571	4.563	4.564	4.605	4.26
0.55	2.927	2.916	2.932	2.963	2.55	5.005	4.985	5.015	5.006	4.64
0.50	3.233	3.210	3.255	3.294	2.82	5.528	5.489	5.66	5.6316	5.10
0.45	4.085	4.077	3.675	3.716	3.12	6.984	6.977	6.268	6.355	5.67
0.40	5.090	5.060	4.220	4.262	3.53	8.704	8.654	7.215	7.340	6.38

Calculations shown in Table III are for different viscosity ratios and a value of $\bar{b}_3 = 0.01$ cm. Neither R_{SD} nor R_{UD} are expected to be a function of $\bar{b}_3$. This is supported by calculations for other $\bar{b}_3$ values not shown here. It is clear from this table that as the dispersed phase volume concentration increases the expected per cent error is also increased if one replaces the size distributed cloud surrounding the test drop (or bubble) by a cloud of uniform sized drops (or bubbles) of size $\bar{b}_{32}$. This behaviour is reasonable because at the lower dispersed phase concentrations the effect of disturbances due to other drops (or bubbles) is reduced as the inter-drop distances has become very large. Therefore the effect of the size distribution in the other drops (or bubbles on the test drop is muted at low volume concentrations. If the test drop has a size other than the Sauter mean radius, $\bar{b}_{32}$, the expected per cent error in R_{UD} changes significantly even if the cloud concentration and Sauter mean radius of the cloud remain same. The effect seems to be insignificant for test drops smaller than the size $\bar{b}_{32}$. However, as the test drop size increases relative to $\bar{b}_{32}$, the expected percent error in R_{UD} increases significantly. When the viscosity ratio, f is less than one, the expected per cent error in R_{UD} was found to be maximum at higher dispersed phase volume fraction for the test drops (or bubbles) of highest size. On the other hand, for viscosity ratio higher than one the expected error in R_{UD} was found to be maximum with the highest

size test drops (or bubbles'at lower dispersed volume fractions.

These tables indicate further that there is no case in which the expected per cent error in R_{UD} is more than 6 per cent when compared to R_{SD}. Thus the analysis confirms that if a size distributed cloud is replaced by a cloud of uniform sized drops of size equal to $\bar{b}_{32}$ of the size distributed cloud, the results would not be much different from that derived by using a cloud of size distributed drops (or bubbles). The same conclusion was obtained by Gal-Or and Hoelscher [15] on the basis of an inadequate expression for mass transfer coefficient to a drop as pointed out earlier.

No experimental data on drops or bubbles is available to check the above theoretical conclusions. However, Tan et al.[32] made measurements of mass transfer coefficient in a 5 cm long packed bed section of active size distributed spheres. This section was preceded by a 10 cm section of inert spheres having the same size distribution. Tan et al. [32] concluded that their data from Re=2 to 1000 was adequately correlated by the following expression due to Karabelas et al.[28] obtained with an inactive cloud of uniform spheres

$$\epsilon(Sh)(Sc^{-1/3}) = \left\{ [1.1\ Re^{1/3}]^4 + [0.29\ Re^{2/3}]^4 \right\}^{1/4} \tag{6.1}$$

if the Sauter mean diameter $2\bar{b}_{32}$ of the size distributed spheres is used in the correlation (6.1) developed with uniform spheres. Since the depth of the active packed zone is only 5 cm and the Sauter mean diameter of each of the size distributions

used is around 1.50 cm or more (Table I of Tan et al.[32]),
we may assume that the active section is very shallow and that
the mass transfer analysis for an inactive cloud of spherical
particles of Sirkar [12] will be applicable here. The relevant
equation is

$$(Sh)(Sch)^{-1/3} = \frac{0.992(1+a\bar{b}_{32})^{1/3}}{\varepsilon^{1/3}} (Re)^{1/3} \quad (6.2)$$

where the particle Reynolds number Re is defined with respect
to the superficial velocity U_{su} in a packed bed so that this
mass transfer asymptote for creeping flow is valid up to a
particle Re = $(U_{su} 2 \bar{b}_{32}/\gamma) < 10$ [12]. In Table IV, with the
help of the size distribution function, (5.48), values of $(Sh)^{-1/3}$
have been calculated for all the four mixtures of Tan et al.[32]
at two values of Re=2 and 10 for a few values of void volume
fraction $\varepsilon(=1-c)$. The values of $\varepsilon(Sh)(Sc)^{-1/3}$ from an enlarged
Figure 2 of Tan et al.[32] for Re=2,10 have been obtained and
recalculated as $(Sh)(Sc)^{-1/3}$ in Table IV. One notices, first,
that up to an $\varepsilon=0.5$, the predicted values of $(Sh)(Sc)^{-1/3}$ for
the four different mixtures are very close to one another. The
deviations between the predictions for mixtures 1 and 2 on the
one hand and those for mixtures 3 and 4 on the other hand go
beyond 10 per cent as the void volume fraction decreases below
0.45. It is known [12] that solutions based on Tam's [6]
approach become increasingly inexact in this range of void
volume fractions. Thus the data of Tan et al.[32] provide a
limited verification for the theoretical conclusions of this
study.

It may be further observed from Table IV that the values
of $(Sh)(Sc)^{-1/3}$ from the data of Tan et al. [32] seem to be
somewhat lower than the calculated values shown in Table IV.
The deviation increases as the void volume fraction decreases
to a value of 0.4. This behaviour is also due to the increasing
inexactness in solutions based on Tam's [6] velocity profile
which blows up when $\varepsilon \rightarrow 1/3$. However, the deviations for ε in
the range of 0.5 to 0.7 are less than 10 per cent.

Analytical expression (5.26A) has been obtained for the
expected Sherwood number as a function of Peclet numbers in
creeping flow around a round test drop (or bubble) placed in
an ensemble of round drops (or bubbles) having an arbitrary
size distribution by utilising the velocity profile derived
by Sirkar [19] on the basis of point force approximation and
other assumptions of Tam [6]. In the limit of a single drop
(or bubble) placed in an infinite fluid this expression (5.26A)
reduces to that of Levich [23]. The expected value of the
quantity $Sh\ Pe^{-1/2}$ in a cloud of uniform sized drops was found
to be substantially lower than that predicted by Gal-Or and
Waslo[17] except at high volume concentration of drops. The latter
conditions are encountered in the limit of dispersed phase holdup
fraction approaching 2/3 when the present solution breaks down
since the assumptions of no drop-drop (or bubble-bubble)
correlation in Sirkar's [19] derivation of velocity profile
through the cloud of drops (or bubbles) are no longer valid.

Further this demonstrates the magnitude of possible error in the mass transfer coefficient if one replaces the size distributed population of drops (or bubbles) by a uniform sized population of drops (or bubbles) of size $\bar{b}_{32}$. It was shown that error is usually small (less than 6 per cent) in all possible cases for the creeping flow regime with no surfactants being present.

SUGGESTIONS FOR FUTURE WORK

1. It would be useful to make experimental measurements in the manner of Karabelas et al. [28] of the mass transfer coefficient to a single active spheroidal particle in a packed bed of similar inactive particles with all of them having the same orientation. The variation of the eccentricity ratio will be particularly desirable. Such measurements may also be attempted in an expanded bed. High Schmidt number conditions are to be maintained and natural convection should be eliminated for this viscous transport problem.

2. It would be worthwhile to develop the equations of motion for viscous flow around a test spheroidal particle in a cloud of size distributed spheroidal particles with the help of the point force approximation of Tam [6] and investigate the possibilities of getting its solution since its boundary conditions are similar to those for a stationary spheroid in a fluid moving with a uniform velocity at infinity.

3. Since nonspherical bubbles are often encountered in industrial practice, it would be useful to model the motion for a spheroidal drop and obtain estimates for its Sherwood number in viscous flow.

REFERENCES

1. Neale, G. and Nader,W.K. 'Prediction of Transport Processes with Porous Media', AIChE Journal, 22, 182 (1976).

2. Buckles, R.G., E.G.,E.W. Merrill and E.R. Gilland, 'An Analysis of Oxygen Absorption in Tubular Membrane oxygenator', AIChE J., 14, 703 (1968).

3. Chilcote, D.D. 'The Diffusion of Ions in Agar Gel Suspensions of Red Blood Cells', Ph.D.Thesis, Cal. Inst. Technol., Pasadena (1971).

4. Colton, C.K., K.A. Smith,E.Q. Merrill and S. Friedman, 'Diffusion of Area in Flowing Blood', AIChE J., 17, 800 (1971).

5. Happel, J., AIChE J., 4, 197 (1958).

6. Tam, C.K.W., J. Fluid Mechanics, 38, 537 (1969).

7. Childress, S., J. Chem. Phys. 56, 2527 (1972).

8. Lundgren, T.S., J. Fluid Mech. 51(2), 273 (1972).

9. Batchelor, G.K., J. Fluid Mech. 52(2), 273 (1972).

10. Jeffery, G.B., Proc. Roy. Soc. (London), A102, 161 (1922).

11. Pfeffer,R., Ind. Eng.Chem.Fund. 3 380 (1964).

12. Sirkar, K.K., Chem. Engng. Sci. 29, 863 (1974).

13. Lightfoot, E.N., AIChE Continuing Education Series (4), Lectures in Transport Phenomena,AIChE, New York (1969).

14. Stewart, W.E., AIChE, J. 9 528 (1963).

15. Gal-Or, B., and Hoelscher, H.E., AIChE J., 12, 499(1966).

16. Gal-Or, B., and Waslo, S., Chem.Engng. Sci., 23, 1431 (1968).

17. Waslo, S., and Gal-Or, B., ibid 16 39 (1971).

18. Happel, J. and Brenner, H., Low Reynold Number Hydrodynamics, Prentice-Hall, Inc., Englewood Cliffs, N.J. (1965).

19. Sirkar, K.K., Chem.Engng. Sci. 32 (10), 1127 (1977).

20. Olney, R.B., AIChE J., 10, 827 (1964).

21. Levich,V.G., Physicochemical Hydrodynamics, Prentice-Hall, Englewood Cliffs, N.J., 1962.

22. Cunningham, E., Proc. Royal Soc. (London), A83, 357 (1910).

23. Soffman, P.G., Stud. Appl. Math. 52(2) 115 (1973).

24. Padmanabhan, L. and Gal-Or, B., Chem.Engng. Sci. 23 631 (1968).

25. Richardson, J.F. and Zaki, W.N., Trans. Instn. Chem. Engrs. 32 35 (1954).

26. Tardos,G.I. Gutfinger, C. and Abuaf, N., AIChE J., 22 1147 (1976).

27. Neale, G. and Nader,W.K., AIChE J., 20, 530 (1974).

28. Karabelas, A.J.,Wegner, T.H. and Hanratty, T.J., Chem. Eng. Sci. 26, 1581 (1971).

29. Wilson,E.J., and Geankoplis, C.J., Ind. Eng. Chem. Fundamentals, 5, 9 (1966).

30. Yaron, I. and Gal-Or, B., Int. J. Heat Mass Transfer 14 727 (1971).

31. Gal-Or, B. and Resnick, W., Chem. Engng. Sci. 19 653 (1964).

32. Tan, A.Y., Prasher, B.D. and Guin, J.A., AIChE J., 21 396 (1975).

33. Thoenes, D., and Kramers, H., Chem.Engng. Sci. 8 271 (1958).

APPENDIX A

DRAG ON A BODY

The second rank (dyadic) stress tensor, $\overline{\overline{\Pi}}$, for Newtonian fluids, is given by

$$\overline{\overline{\Pi}} = -P\,\overline{\overline{I}} + K\,(\nabla \cdot \overline{V})\,\overline{\overline{I}} + 2\,\mu\,\overline{\overline{\Delta}} \qquad (A.1)$$

where P = the hydrostatic pressure the fluid would be

supporting if it were at rest at its local

density and temperature, T.

$\overline{\overline{I}}$ = unit tensor

K = bulk or volume viscosity

μ = shear viscosity

$\overline{\overline{\Delta}}$ = rate of deformation tensor, defined in Eq.(A.3)

For compressive fluids the pressure p which appears in equation (A.1) is not the mean normal pressure, P_m, at any point. The mean pressure P_m is defined as follows:

$$P_m = -\frac{1}{3}\,\overline{\overline{\Pi}} : \overline{\overline{I}}$$

$$= -\frac{1}{3}\,(\overline{\overline{\Pi}}_{xx} + \overline{\overline{\Pi}}_{yy} + \overline{\overline{\Pi}}_{zz})$$

(for a Cartesian coordinate system)

$$P_m = P - K\,(\overline{\overline{\nabla}} \cdot \overline{V}) \qquad (A.2)$$

The term, $\overline{\overline{\Delta}}$, in equation (A.1) is based on a linear relationship between the viscous portion of the

pressure tensor and the rate of deformation (shear) tensor. This leads to

$$\overline{\overline{\triangle}} = \frac{1}{2} [\nabla \bar{v} + (\nabla\bar{v})^t] - \frac{1}{3}\overline{\overline{I}}(\nabla\bar{v}) \tag{A.3}$$

where $(\nabla \bar{v})^t$ = transpose of $\nabla \bar{v}$.

For an incompressible fluid, the equations (A.1) and (A.3) can be written in more simplified form as follows:

$$\overline{\overline{\Pi}} = - P \overline{\overline{I}} + 2\mu \overline{\overline{\triangle}} \tag{A.4}$$

and

$$\overline{\overline{\triangle}} = \frac{1}{2} [\nabla \bar{v} + (\nabla \bar{v})^t] \tag{A.5}$$

We shall adopt the orthogonal curvilinear coordinate system for an axisymmetric body. The notations for the coordinate system are same as those in Chapter 2.

Thus for an axisymmetric body

$$h_\beta = h_\eta = h \tag{A.6}$$

and

$$h_\varphi = \frac{1}{w} \tag{A.7}$$

For our coordinate system (see page 489, Happel and Brenner [18]).

$$\nabla \bar{v} = \bar{i}_\beta \, \bar{i}_\beta \, h \left[\frac{\partial v_\beta}{\partial \beta} - h \, v_\eta \frac{\partial}{\partial \eta} \left(\frac{1}{h} \right) \right]$$

$$+ \bar{i}_\beta \, \bar{i}_\eta \, h \left[\frac{\partial v_\eta}{\partial \beta} - h \, v_\beta \frac{\partial}{\partial \eta} \left(\frac{1}{h} \right) \right]$$

$$+ \bar{i}_\eta \, \bar{i}_\beta \, h\left[\frac{\partial v_\beta}{\partial \eta} - h \, v_\eta \frac{\partial}{\partial \beta}\left(\frac{1}{h}\right)\right]$$

$$+ \bar{i}_\eta \, \bar{i}_\eta \, h\left[\frac{\partial v_\eta}{\partial \eta} + h \, v_\beta \frac{\partial}{\partial \beta}\left(\frac{1}{h}\right)\right]$$

$$+ \bar{i}_\varphi \, \bar{i}_\varphi \, h_\varphi\left[h \, v_\beta \frac{\partial}{\partial \beta}\left(\frac{1}{h_\varphi}\right) + h \, v_\eta \frac{\partial}{\partial \eta}\left(\frac{1}{h_\varphi}\right)\right] \qquad (A.8)$$

$$(\nabla \bar{v})^t = \bar{i}_\beta \, \bar{i}_\beta \, h\left[\frac{\partial v_\beta}{\partial \beta} + h \, v_\beta \frac{\partial}{\partial \eta}\left(\frac{1}{h}\right)\right]$$

$$+ \bar{i}_\beta \, \bar{i}_\eta \, h\left[\frac{\partial v_\beta}{\partial \eta} - h \, v_\eta \frac{\partial}{\partial \beta}\left(\frac{1}{h}\right)\right]$$

$$+ \bar{i}_\eta \, \bar{i}_\beta \, h\left[\frac{\partial v_\eta}{\partial \beta} - h \, v_\beta \frac{\partial}{\partial \eta}\left(\frac{1}{h}\right)\right]$$

$$+ \bar{i}_\eta \, \bar{i}_\eta \, h\left[\frac{\partial v_\eta}{\partial \eta} + h \, v_\beta \frac{\partial}{\partial \beta}\left(\frac{1}{h}\right)\right]$$

$$+ \bar{i}_\varphi \, \bar{i}_\varphi \, h_\varphi\left[h \, v_\beta \frac{\partial}{\partial \beta}\left(\frac{1}{h_\varphi}\right) + h \, v_\eta \frac{\partial}{\partial \eta}\left(\frac{1}{h_\varphi}\right)\right]$$

$$(A.9)$$

Substitution of $(\nabla \bar{v})$ and $(\nabla \bar{v})^t$ from (A.8) and (A.9) respectively into (A.5) leads to

$$\bar{\bar{\Delta}} = \bar{i}_\beta \, \bar{i}_\beta \, h\left[\frac{\partial v_\beta}{\partial \beta} + h \, v_\eta \frac{\partial}{\partial \eta}\left(\frac{1}{h}\right)\right]$$

$$+ \bar{i}_\beta \bar{i}_\eta \, \frac{h}{2}\left[\frac{\partial v_\eta}{\partial \beta} + \frac{\partial v_\beta}{\partial \eta} - h \, v_\beta \frac{\partial}{\partial \eta}\left(\frac{1}{h}\right)\right.$$

$$\left. - h \, v \frac{\partial}{\partial \eta}\left(\frac{1}{h}\right)\right]$$

$$+ \bar{i}_\eta \, \bar{i}_\eta \, h\left[\frac{\partial v_\eta}{\partial \eta} + h \, v_\beta \frac{\partial}{\partial \beta}\left(\frac{1}{h}\right)\right]$$

$$+ \bar{i}_\varphi \bar{i}_\varphi \, h_\varphi\left[h \, v_\beta \frac{\partial}{\partial \beta}\left(\frac{1}{h}\right) + h \, v_\eta \frac{\partial}{\partial \eta}\left(\frac{1}{h_\varphi}\right)\right.$$

$$+\bar{i}_\eta\bar{i}_\beta \cdot \frac{h}{2}\left[\frac{\partial v_\beta}{\partial \eta} + \frac{\partial v_\eta}{\partial \beta} - hv_\eta \frac{\partial}{\partial \beta}\left(\frac{1}{h}\right) - h \, v_\beta\frac{\partial}{\partial \eta}\left(\frac{1}{h}\right)\right] \qquad (A.10)$$

The stress vector acting across an element of surface area whose outer normal is $\bar{i}_\beta$, shall be of the form

$$\overline{\overline{\Pi}}_\rho = \overline{\overline{\Pi}}.\overline{i}_\rho = (-P\,\overline{\overline{I}} + 2\mu\,\overline{\overline{\triangle}})\,.\,\overline{i} \qquad\qquad (A.11)$$

The unit tensor, $\overline{\overline{I}}$, is given by

$$\overline{\overline{I}} = \overline{i}_\rho\,\overline{i}_\rho + \overline{i}_\eta\,\overline{i}_\eta + \overline{i}_\varphi\,\overline{i}_\varphi \qquad\qquad (A.12)$$

Substitution of $\overline{\overline{\triangle}}$ and $\overline{\overline{I}}$ from (A.10) and (A.12) respectively into (A.11) and further simplification leads to

$$\overline{\overline{\Pi}}_\rho = -\overline{i}_\rho P + 2\mu h[\ \overline{i}_\rho\,\frac{\partial v_\rho}{\partial\rho} + i_\eta\,\frac{\partial v_\rho}{\partial\eta}\ ]$$

$$+ i_\eta\,\mu\,h^2[\frac{\partial}{\partial\rho}\,(\frac{v_\eta}{h}) - \frac{\partial}{\partial\eta}\,(\frac{v_\rho}{h})]$$

$$+ 2\mu\,v_\eta\,[i_\eta\,\frac{\partial h}{\partial\rho} - \overline{i}_\rho\,\frac{\partial h}{\partial\eta}] \qquad\qquad (A.13)$$

The general properties of any vector leads to the following two relations:

$$\nabla\,v_\rho = \overline{i}_\rho\,h\,\frac{\partial v_\rho}{\partial\rho} + \overline{i}_\eta\,h\,\frac{\partial v_\rho}{\partial\eta} \qquad\qquad (A.14)$$

and

$$\text{Curl }\overline{V} = \overline{i}_\varphi\,h^2\,[\frac{\partial}{\partial\rho}\,(\frac{v_\eta}{h}) - \frac{\partial}{\partial\eta}\,(\frac{v_\rho}{h})]$$

$$\overline{i}_\varphi.(\text{curl }\overline{V}) = h^2[\frac{\partial}{\partial\rho}\,(\frac{v_\eta}{h}) - \frac{\partial}{\partial\eta}\,(\frac{v_\rho}{h})]$$

where $\overline{V}$ has three components v_ρ, v_η and v_φ (=0).

Using equations (A.14) and (A.15), the stress vector defined by equation (A.13) reduces to

$$\overline{\overline{\Pi}}_\rho = -\overline{i}_\rho P + 2\mu\,\nabla\,v_\rho + \overline{i}_\eta\,\mu\,[\overline{i}_\varphi\cdot(\text{curl }\overline{V})]$$

$$+ 2\mu\,v_\eta\,[\overline{i}_\eta\,\frac{\partial h}{\partial\rho} - \overline{i}_\rho\,\frac{\partial h}{\partial\eta}] \qquad\qquad (A.16)$$

Happel and Brenner [18] have derived the following relations for a axisymmetric body

Vorticity vector = Curl $\bar{V}$

$$\text{Curl } \bar{V} = \nabla \times \bar{V} = \frac{i_\varphi}{w} E^2 \psi \tag{A.17}$$

Finally, the relations (2.41), (2.42) and (A.17), connecting the normal velocity, tangential velocity and the vorticity, respectively, to the stream function, leads to the following stress vector:

$$\overline{\overline{\Pi}}_\rho = -\bar{i}_\rho P - 2\mu \nabla \left(\frac{h}{w} \frac{\partial \psi}{\partial \eta} \right) + \bar{i}_\eta \mu \left(\frac{1}{w} E^2 \psi \right)$$

$$+ \frac{2 \mu h}{\bar{w}} \left(\frac{\partial \psi}{\partial \rho} \right) \left[\bar{i}_\eta \frac{\partial h}{\partial \rho} - \bar{i}_\rho \frac{\partial h}{\partial \eta} \right] \tag{A.18}$$

The force exerted on the body by the fluid in the positive z-direction will be

$$F_z = \int_{\substack{S=\text{Surface} \\ \text{of the body}}} \overline{\overline{\Pi}}_z \cdot d\bar{S} = \int_S \overline{\overline{\Pi}}_z \cdot \bar{i}_\rho \, dS$$

$$= \int_S \Pi_{z\rho} \, dS = \int_S \Pi_{\rho z} \, dS$$

$$= \int_0^{2\pi} \int \overline{\Pi}_{\rho z} \frac{\bar{w}}{h} \, d\eta \, d\varphi$$

$$F_z = 2\pi \int \Pi_{\rho z} \frac{\bar{w}}{h} \, d\eta \tag{A.19}$$

$$\Pi_{\rho z} = \overline{\overline{\Pi}}_\rho \cdot \bar{i}_z = -(\bar{i}_\rho \cdot \bar{i}_z) P - 2\mu (\bar{i}_z \cdot \nabla) \left(\frac{h}{w} \frac{\partial \psi}{\partial \eta} \right)$$

$$+ (\bar{i}_\eta \bar{i}_z) \mu \left(\frac{1}{w} E^2 \right)$$

$$+ \frac{2\mu h}{\bar{w}} \left(\frac{}{\rho} \right) \left[(\bar{i}_\eta \cdot \bar{i}_z) \frac{h}{\rho} - (\bar{i}_\rho \cdot \bar{i}_z) \frac{h}{\eta} \right. \tag{A.20}$$

For relating the coordinates, the following relations hold good:

$$\bar{i}_w \, \bar{i}_\eta = h \frac{\partial \bar{w}}{\partial \eta} = \bar{i}_\beta \, \bar{i}_z \qquad (A.21)$$

and

$$\bar{i}_w \, \bar{i}_\beta = h \frac{\partial \bar{w}}{\partial \beta} = -\bar{i}_\eta \, \bar{i}_z \qquad (A.21)$$

Substitution of $\Pi_{\beta z}$ from (A.20) in to (A.19) with regard to the equation (A.21) and (A.22) leads to the following drag expression

$$F_z = -\pi \int \frac{\partial}{\partial \eta}(\bar{w}^2 P)\, \delta\eta + \pi \int \bar{w}^2 \frac{\partial P}{\partial \eta}\, \delta\eta$$

$$-2\pi\mu \int \frac{\partial}{\partial \eta}(\bar{w}\cdot\bar{v}_w)\, \delta\eta - 2\pi\mu \oint E^2 \psi \frac{\partial w}{\partial \beta}\, \delta\eta$$

$$-4\pi\mu \int h \frac{\partial \psi}{\partial \beta}\left[\frac{\partial \bar{w}}{\partial \beta}\cdot\frac{\partial h}{\partial \beta}+\frac{\partial \bar{w}}{\partial \eta}\frac{\partial h}{\partial \eta}\right]\delta\eta \qquad (A.23)$$

Where the integrals are to be taken around a Meridian section of the body, the end points of the path of integration being the upper and lower points at which the boundary surface intersects the axis of symmetry. Since $\bar{w} = 0$ at these terminal points the first and third integrals vanish identically, leaving

$$F_z = \pi \int \bar{w}^2 \frac{\partial P}{\partial \eta}\, \delta\eta - 2\pi\mu \int E^2 \psi \frac{\partial \bar{w}}{\partial \beta}\, \delta\eta$$

$$-4\pi\mu \int h\left[\frac{\partial \bar{w}}{\partial \beta}\frac{\partial h}{\partial \beta}+\frac{\partial \bar{w}}{\partial \eta}\frac{\partial h}{\partial \eta}\right]\frac{\partial \psi}{\partial \beta}\, \delta\eta \qquad (A.24)$$

Happel and Brenner [18] had developed the relationship between the pressure in steady creeping flow and the stream function as follows:

88

$$\frac{\partial P}{\partial \beta} = \frac{\mu}{\bar{w}} \frac{\partial}{\partial \beta} (E^2 \psi). \tag{A.25}$$

Substitution into the previous expression yields

$$F_z = \pi\mu \int \bar{w}^3 \frac{\partial}{\partial \beta} \left[\frac{E^2 \psi}{\bar{w}^2} \right] \delta\eta$$

$$- 2\pi\mu \int h \frac{\partial \psi}{\partial \beta} \left[\frac{\partial \bar{w}}{\partial \beta} \frac{\partial h}{\partial \beta} + \frac{\partial \bar{w}}{\partial \eta} \frac{\partial h}{\partial \eta} \right] \delta\eta \tag{A.26}$$

This is the most general expression for the force exerted on an axisymmetric body when the continuous phase is an incompressible fluid.

—

APPENDIX B

SIMPLIFICATION OF EXPRESSIONS FOR A SINGLE SPHERE MOVING IN AN INFINITE FLUID MEDIUM

The factor 'G' for a cloud of oblate spheroidal particles is defined by equation (2.32) as follows:

$$G = \text{Sinh } \beta_a + (\text{Sinh}^2\beta_a - 1) [\text{Cot}^{-1} \text{ Sinh}\beta_b - \text{Cot}^{-1} \text{ Sinh } \beta_a] - \frac{\text{Sinh}\beta_b}{\text{Cosh}^2\beta_b} \text{ Cosh}^2\beta_a \qquad (2.32)$$

Equations (2.73) and (2.75) indicate that as the void fraction ε increases, the parameter 'β_b' also increases. For the limiting case of the void fraction ε becoming one, this parameter becomes infinite i.e.

As $\varepsilon \longrightarrow 1.0, \quad \beta_b \longrightarrow \infty$

or $\text{Sinh } \beta_b \longrightarrow \text{Cosh } \beta_b \longrightarrow \infty$

and $\text{Cot}^{-1} \text{ Sinh } \beta_b \longrightarrow 0$

Thus, equation (2.32) reduces to

$$G = \text{Sinh}\beta_a - (\text{Sinh}^2\beta_a - 1) \text{ Cot}^{-1} \text{ Sinh } \beta_a \qquad (B.1)$$

The function $\text{Cot}^{-1} \text{ Sinh } \beta_a$ may be written in the form of a series as follows:

$$\text{Cot}^{-1}\text{Sinh } \beta_a = \frac{1}{\text{Sinh}\beta_a} - \frac{1}{3\,\text{Sinh}^3\beta_a} + \frac{1}{5\,\text{Sinh}^5\beta_a}$$
$$- \frac{1}{7\,\text{Sinh}^7\beta_a} + \dots \qquad (B.2)$$

Substitution of this into the previous expression yields the following equation:

$$G = \frac{1}{\sinh \beta_a} + \frac{1}{3 \sinh \beta_a} - \frac{1}{3 \sinh^3 \beta_a} - \frac{1}{5 \sinh^3 \beta_a}$$

$$+ \frac{1}{5 \sinh^5 \beta_a} + \frac{1}{7 \sinh^5 \beta_a} \ldots \ldots$$

or

$$G = \frac{4}{3} \frac{1}{\sinh \beta_a} - \frac{8}{15} \frac{1}{\sinh^3 \beta_a} + \frac{12}{35} \frac{1}{\sinh^5 \beta_a} \qquad (B.3)$$

Equation (2.76) indicates that the coordinate β_a **tends** to infinity as the ratio b/a approaches unity.

$$\beta_a \longrightarrow \infty \qquad \text{as} \quad \frac{b}{a} \longrightarrow 1$$

and

$$\sinh \beta_a \longrightarrow \infty \qquad \text{as} \quad \frac{b}{a} \longrightarrow 1 .$$ Therefore since $\sinh \beta_a$ is a very large number as $\frac{b}{a} \longrightarrow 1$, we conclude that

$$\sinh^3 \beta_a \ggg \sinh \beta_a \qquad \text{as} \quad \frac{b}{a} \longrightarrow 1$$

or

$$\frac{1}{\sinh \beta_a} \ggg \frac{1}{\sinh^3 \beta_a} \qquad \text{as} \quad \frac{b}{a} \longrightarrow 1 \qquad (B.4)$$

Thus the equation (B.3) can be written with the help of (B.4) in the following form

$$G = \frac{4}{3 \sinh \beta_a} \qquad \text{as} \quad \frac{b}{a} \longrightarrow 1 \qquad (B.5)$$

Substitution of G from (B.5) into (2.36) gives the drag experienced by a sphere moving in an infinite medium as

$$F_z = \frac{9 \pi \mu U C \sinh \beta_a}{\frac{4}{3}} \qquad as \quad \frac{b}{a} \rightarrow 1$$

$$C \sinh \beta_a = r, \text{ radius of sphere}$$

$$\text{when } \frac{b}{a} = 1$$

Thus

$$F_z = 6 \pi \mu U r \tag{B.6}$$

which is the well known Stoke's formula.

The factor $F(\beta_a)$ in equation (3.37) for a oblate spheroidal particle is defined by (3.33) as

$$F(\beta_a) = \frac{\displaystyle\int_0^\pi \frac{\sin^2 \eta}{(\eta - \frac{\sin 2\eta}{2})^{1/3}} \sqrt{(\cosh^2\beta_a - \sin^2\eta)} \, d\eta}{\sinh^{2/3}\beta_a \, \cosh^{2/3}\beta_a [\coth \beta_a + \frac{\sinh \beta_a}{2} \log_e (\frac{\cosh\beta_a + 1}{\cosh \beta_a - 1})]}$$

$$\tag{3.33}$$

or

$$F(\beta_a) = \frac{\cosh^{1/3}\beta_a \displaystyle\int_0^\pi \frac{\sin^2 \eta}{(\eta - \frac{\sin 2\eta}{2})^{1/3}} \sqrt{[1 - (\frac{\sin \eta}{\cosh \beta_a})^2]} \, d\eta}{\sinh^{2/3} \beta_a [\coth \beta_a + \frac{\sinh \beta_a}{2} \log_e (\frac{\cosh \beta_a + 1}{\cosh \beta_a - 1})]}$$

$$\tag{B.7}$$

As we know that

$$\frac{1}{2} \log_e \left(\frac{1 + \frac{1}{\cosh \beta_a}}{1 - \frac{1}{\cosh \beta_a}} \right) = \frac{1}{\cosh \beta_a} + \frac{1}{3 \cosh^3 \beta_a} + \frac{1}{5 \cosh^5 \beta_a} +$$

$$\tag{B.8}$$

Substituting the above into the previous expression yields the following:

$$F(\beta_a) = \frac{Coth^{1/3}\beta_a \int_0^{\pi} \frac{Sin^2\eta}{(\eta - \frac{Sin 2\eta}{2})^{1/3}} \sqrt{[1-(\frac{Sin\eta}{Cosh\,\beta_a})^2]}\, d\eta}{Sinh^{1/3}\beta_a[Coth\beta_a + Tanh\beta_a + \frac{Tanh\,\beta_a}{3\,Cosh^2\beta_a} + \frac{Tanh\,\beta_a}{5\,Cosh^4\beta_a} + \ldots]}$$

(B.9)

Now $\beta_a \longrightarrow \infty$ as $\frac{b}{a} \longrightarrow 1$

and $Sinh\beta_a \longrightarrow Cosh\beta_a \longrightarrow \infty$ as $\frac{b}{a} \longrightarrow 1$

$Tanh\,\beta_a \cong Coth\,\beta_a \cong 1.0$ as $\frac{b}{a} \longrightarrow 1$

and

$$Tanh\,\beta_a \gg \frac{Tanh\,\beta_a}{Cosh^2\,\beta_a}$$

Thus the equation (b.9) can be written for the limiting case of a single sphere in the fluid in the following form:

$$F(\beta_a) = \frac{\int_0^{\pi} \frac{Sin^2\eta}{(\eta - \frac{Sin\,2\eta}{2})^{1/3}}\, d\eta}{2\,Sinh^{1/3}\,\beta_a}$$

(B.10)

$$F(\beta_a) = \frac{1.6103}{2\,Sinh^{1/3}\,\beta_a} = \frac{0.80515}{Sinh^{1/3}\,\beta_a}$$

(B.11)

where the value of the integral in the numerator of (B.10) is available on page 85 of Levich [21].

APPENDIX C

RELATIONSHIP OF OUTER SOLID ENVELOPE AND FREE SURFACE WITH VOID FRACTION FOR THE ASSEMBLAGE OF PARTICLES ARRANGED IN A FIXED GEOMETRY (BCRP)

For lower particle concentrations we may assume that all particles are uniformly distributed and are spaced according to the well known Body Centered Cubic Structure for spheres. For such an assemblage of oblate (or prolate) spheroidal particles, we assume that the particles are spaced according to the BodyCentered Rectangular Parallelepiped (BCRP) unit cell as shown in Figure 6 such that only the free surface of each particle touches the free surface of another particle, while the particles are not in direct contact with each other.

Here we define

$$1-\bar{\varepsilon} = \frac{\text{Dispersed phase volume per unit BCRP cell}}{\text{Volume of BCRP unit cell}}$$

$$1-\bar{\varepsilon} = \frac{V_s}{V} \tag{C.1}$$

Two unequal arms l_s and l_m of BCRP unit cell will be in the same ratio as that of the minor to major axis of the oblate (or prolate) spheroidal free surface:

$$\frac{l_s}{l_m} = \frac{C.\ \sinh \beta_f}{C\ \cosh \beta_f}$$

or

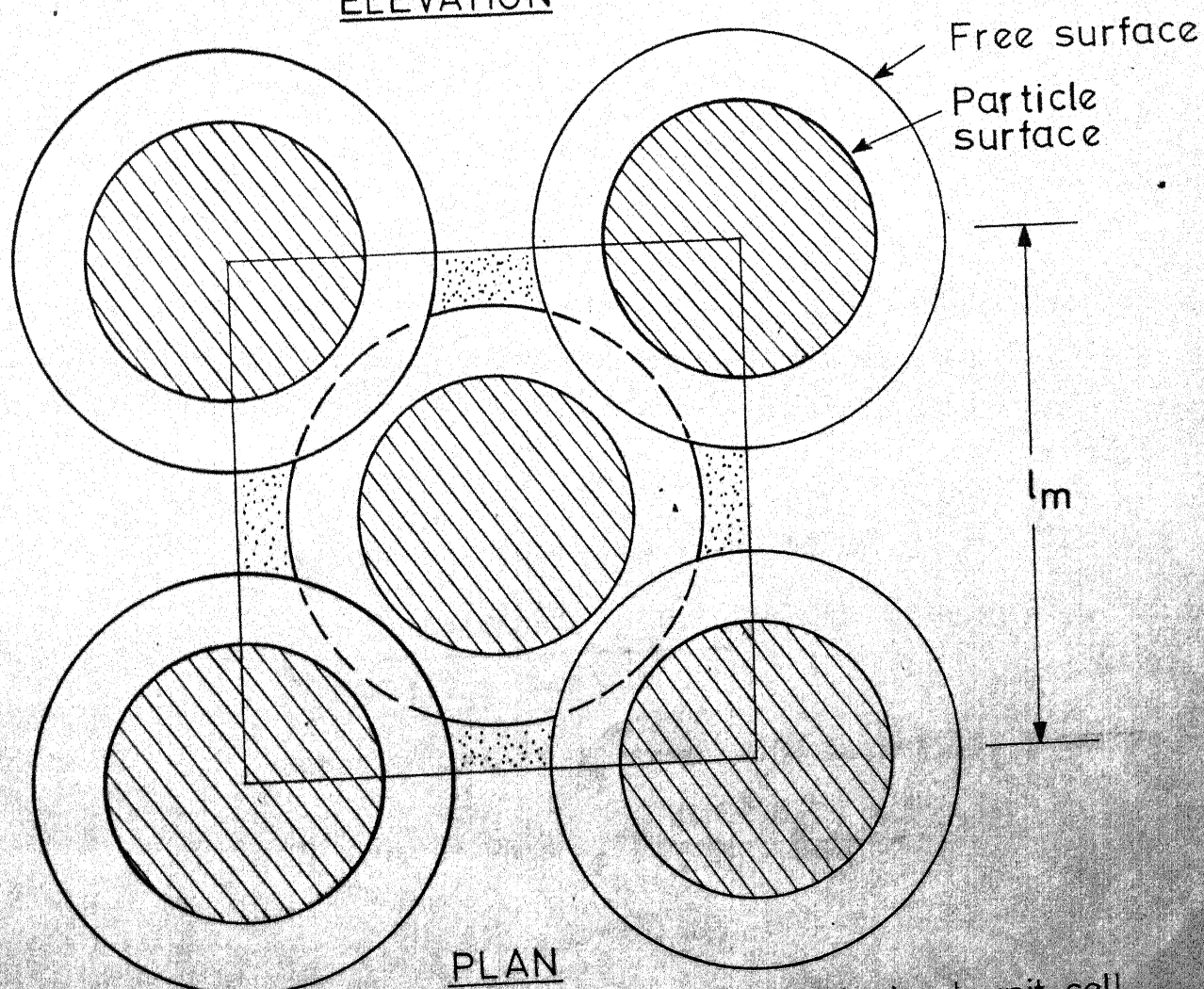Free surface

Particle surface

l_s

l_m

ELEVATION

Free surface

Particle surface

l_m

PLAN
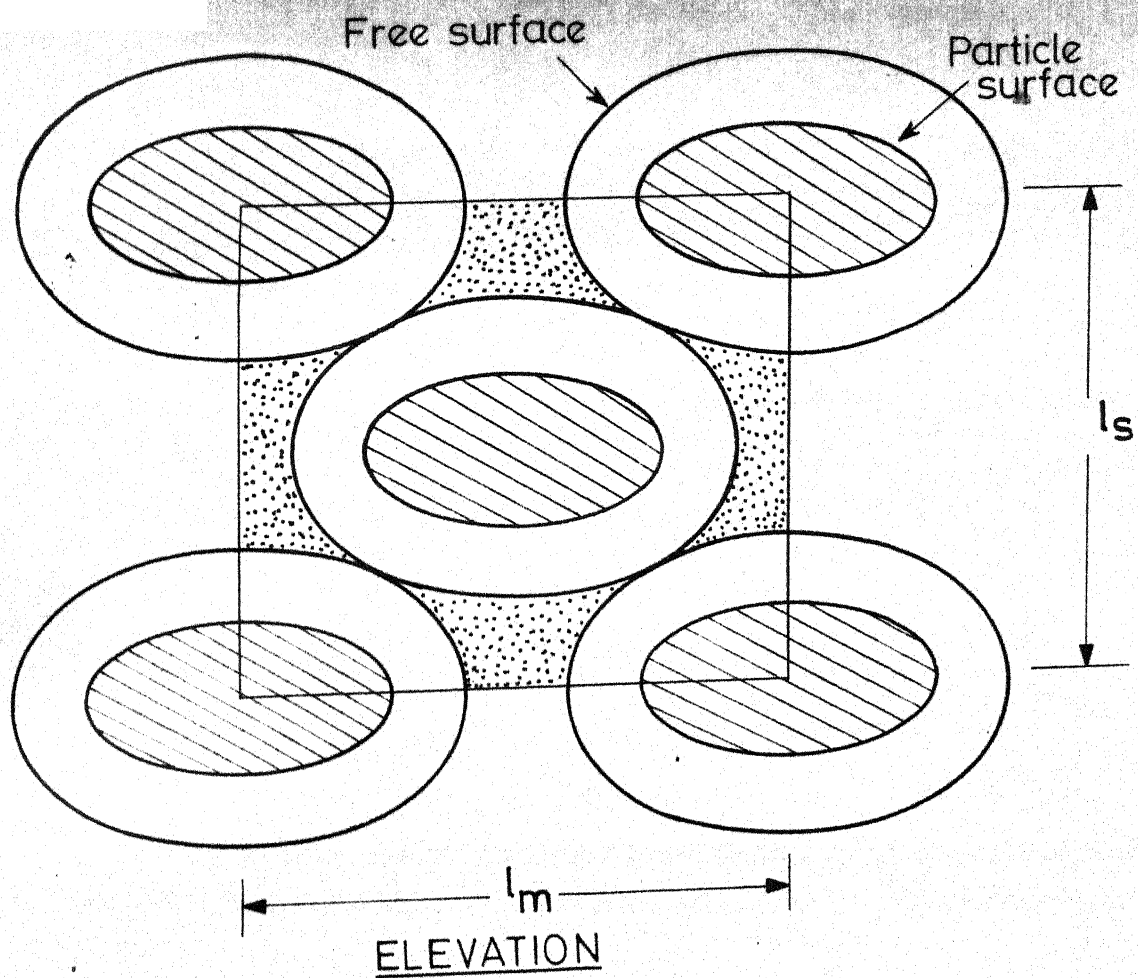
Fig. 6 Body centered rectangular parallelepiped unit cell

$$l_s = l_m \; \text{Tanh} \; \beta_f \tag{C.2}$$

Volume of BCRP unit cell is given by

$$V = l_m^2 \; l_s$$

using (C.2)

$$V = l_m^3 \; \text{Tanh} \; \beta_f \tag{C.3}$$

Distance D_e between the centers of two neighbouring free surface envelopes is equal to two times the distance between the centre and the point of contact of a free surface envelope. Thus

$$D_e = 2 \; C\sqrt{(\text{Sinh}^2 \; \beta_f + 0.5)} \tag{C.4}$$

D_e = half of the diagonal of the BCRP cell

$$= \tfrac{1}{2}\sqrt{(l_s^2 + l_m^2 + l_s^2)}$$

This reduces to the following on substitution of l_s from (C.2)

$$D_e = \frac{l_m}{2} \sqrt{(2 + \text{Tanh}^2 \beta_f)} \tag{C.5}$$

By equating (C.4) and (C.5) we get

$$l_m = \frac{4 \; C\sqrt{(\text{Sinh}^2\beta_f + 0.5)}}{\sqrt{(2 + \text{Tanh}^2 \; \beta_f)}} \tag{C.6}$$

Substitution of l_m from (C.6) into (C.3) leads to

$$V = 64 \; C^3 \; \text{Tanh} \; \beta_f \; \left[\frac{\text{Sinh}^2 \; \beta_f + 0.5}{2.0 + \text{Tanh} \; \beta_f} \right]^{3/2} \tag{C.7}$$

Each corner free surface envelope does not belong uniquely to one unit cell, but is a part of all eight unit cells surrounding it. Therefore only one eight part of each corner free surface envelope belongs to one unit cell. Each cell also possesses a free surface envelope located at its center that is not shared with any other unit cells. Thus BCRP unit cell has two free surface envelope; one contributed by the eight corner free surface envelopes and one located at its center. In other words we can say that there are two oblate spheroidal particles per BCRP unit cell.

Thus volume of solid phase per BCRP unit cell is

$$V_s = 2 \times \frac{4}{3} \pi \, C^3 \, \text{Sinh} \, \beta_a \, \text{Cosh}^2 \, \beta_a \qquad (C.8)$$

Substituting V_s and V from (C.8) and (C.7) into (C.1) leads to

$$\text{Tanh} \, \beta_f \left[\frac{\text{Sinh}^2 \, \beta_f + 0.5}{2 + \text{Tanh} \, \beta_f} \right]^{3/2} = \frac{\pi}{24} \times \frac{\text{Sinh} \, \beta_a \, \text{Cosh}^2 \, \beta_a}{(1 - \bar{\varepsilon})} \qquad (C.9)$$

For prolate spheroidal particles assemblage the same relationship may be obtained in the following form:

$$\text{Coth} \, \beta_f \left[\frac{\text{Sinh}^2 \beta_f + 0.5}{2 + \text{Coth} \, \beta_f} \right]^{3/2} = \frac{\pi}{24} \times \frac{\text{Cosh} \, \beta_a \, \text{Sinh}^2 \, \beta_a}{(1 - \bar{\varepsilon})} \qquad (C.10)$$

Thus the equation (2.73), (2.76) and (C.9(10))
provide the relationship between β_b and void fraction
of the assemblage of an oblate (or prolate) spheroidal
particles having a particular value of the eccentricity
(b/a) of the spheroid.

At higher particle concentration this BCRP model
will not predict the correct void fraction because the
probability of violating the basic assumption of BCRP model
that the particles are not in direct contact increases as
the particle concentration increases.

```
***************************** **********************************
    CCMPUTER PRCGRAN FOR ESTIMATING THE FACTORS,SMALL A( DEFINED BY
    EQUATION  5.11A  OF THIS THESIS)    FOR SIZE DISTRIBUTED CLCUD OF
    BUBBLES(OR   CROPS),AB32(DEFINED BY EQUATION   5.43 OF THIS  THESIS)
    FOR   UNIFORN  SIZE CLOUD OF BUBBLES(DROPS) AND TO FIND THE PCSSIBLE
    ERRCR IN THE  PRECICTION OF MASS TRANSFER COEFFIENT IF THE SIZE
    DISTRIBUTED CLOUD IS REPLACEC BY A UNIFORM SIZED CLOUD HAVING THE
    SAME  SAUTER MEAN   RADIUS

***************************** **********************************
      DIMENSION  UV(20),BV(20),BA(20),AF(20),AI(20)
      REAC  1,(AF(I),I=1,5)
  1  FORMAT(5F10.5)
      B3=0.1
      PRINT  20
  2  A=0.0
      ALPHA=SCRT(3.14)*B3*B3*B3
      ALPHA=(4.0/ALPHA)**0.666
      BLPHA=(ALPHA**3)/3.14
      BLPHA=SCRT(BLPHA)*4.0
      B=B3/10.
      SI=B
      BA(1)=B-SI
      DO  5  I=2,4
      BA(I)=BA(I-1)+SI
      AI(I)=BLPHA*(BA(I)**5)*EXP(-ALPHA*BA(I)*BA(I))
  5  CONTINUE
      A=A+(AI(2)+4.0*AI(3)+AI(4))*SI/3.
      IF(BA(4)-5.*B3)  10,10,15
 10  B=BA(4)
      GO  TO  4
 15  A=A**0.333
      PRINT  21,B3,A
 20  FORMAT(//,2X,*B3 ASSUMED*,3X,*B3 CALCU*)
 21  FORMAT(//,2X,E10.5,3X,E10.51)
      X=ABS(B3-A)
      Y=B3/100.
      IF(X-Y)  25,25,22
 22  BB=A
      GO  TO  2
 25  UI=0.0
      BI=0.0
      B=B3/10.
      BA(1)=B-SI
      DO27I=2,4
      BA(I)=BA(I-1)+SI
      UV(I)=(BA(I)**5)*EXP(-ALPHA*BA(I)*BA(I))
      BV(I)=UV(I)/BA(I)
      UI=UI+(UV(2)+4.0*UV(3)+UV(4))*SI/3.0
      BI=BI+(BV(2)+4.0*BV(3)+BV(4))*SI/3.0
      IF(BA(4)-5.0*B3) 28,29,29
 28  B=BA(4)
      GO  TO 26
 29  B32=UI/BI
      X=B32/B3
      PRINT  30,X
 30  FORMAT(//,*RATIO OF B32 ANC B3 = *,F8.4)
      PRINT 35
 35  FORMAT(7X,*F*,16X,*C*,16X,*A*,15X,*RS1*,14X,*RS2*,14X,*AB32*)
      A1=1.5
      A2=2.5
      DO 500 K=1,5
      F=AF(K)
      AB32=0.0
```

```
      C=0.05
      BLPHA=18.0*C*SQRT((ALPHA**3)/3.14)/(B3**3)
      A=A1
      GO TO 90
      A=A2
      UI=0.0
      B=B3/10.0
      BA(1)=B-SI
      DO 100 I=2,4
      BA(I)=BA(I-1)+SI
      AB=A*BA(I)
      X=1.0+AB+AN
      X=1.0+AB+AB*AB/3.0+(2.0/3.0+2.0*AB/3.0+AB*AB/3.0+(AB**3)/9.)*F
      Y=1.0+F*(1.0+AB/3.0)
      X=X/Y
      Y=ALPHA*BA(I)*BA(I)
      UV(I)=X*(BA(I)**3)*EXP(-Y)
      UI=UI+(UV(2)+4.0*UV(3)+UV(4))*SI/3.0
      IF(BA(4)-5.*B3) 115,120,120
      B=BA(4)
      GO TO 99
      UI=BLPHA*UI
      UI=SQRT(UI)
      X=UI-A
      IF(A-A1) 121,122,121
      X11=X
      GO TO 86
      X22=X
      IF(ABS(X11)-ABS(X22)) 126,123,125
      A2=A2/2.0
      GO TO 86
      A=A1
      A1=A2
      A2=A
      X=X11
      X11=X22
      X22=X
      IF(ABS(X11)-A1/50.0) 130,130,127
      A2=A2-(A1-A2)*X22/(X11-X22)
      GO TO 86
      A=A1
      B=B3/10.0
      UI=0.0
      BI=0.0
      BA(1)=B-SI
      DO 150 I=2,4
      BA(I)=BA(I-1)+SI
      AB=A*BA(I)
      W=1.+AB+AB*AB/3.+(1.0+AB+AB*AB/2.+(AB**3)/6.0)*2.0*F/3.
      X=(1.0+AB)*BA(I)
      X=SQRT(X/W)
      X=X*BA(I)
      UV(I)=X*  EXP(-ALPHA*BA(I)*BA(I))
      UV(I)=UV(I)*(BA(I)**3)
      BV(I)=BA(I)*.EXP(-ALPHA*BA(I)*BA(I))
      BV(I)=BV(I)*(BA(I)**3)
      CONTINUE
      UI=UI+(UV(2)+4.*UV(3)+UV(4))*SI/3.0
      BI=BI+(BV(2)+4.0*BV(3)+BV(4))*SI/3.0
      IF (BA(4)-5.0*B3)  155,160,160
      B=BA(4)
      GO TO 140
      RS1=UI/BI
      AA=F*(1.0-1.5*C)/3.0
      BB=(1.0+F)*(1.0-1.5*C)
      CC=(6.0+4.0*F)*3.0*C /4.0
      X=AB32
      FX=AA*(X**3)+BB*X*X-CC*(X+1.0)
      IF(FX) 172,176,173
      X=X+0.05
```

```
      GO TC 170
173   X=X-C.05/2.0
174   FX=AA*(X**3)+BB*X*X-CC*(X+1.0)
      FXX=3.0*AA*X*X+2.0*BB*X-CC*X
      Z=FX/FXX
      IF (ABS(Z)-X/10.0) 176,176,175
175   X=X-Z
      GO TC 174
176   AB32=X
      Y=(1.0+AB32)*B32
      W=AB32
      W=1.0+W+W*W/3.0+(1.0+W+W*W/2.0+(W**3)/6.0)*2.*F/3.0
      Y=Y/W
      Y=SQRT(Y)
      RS2=Y
      ZZZ=ABS(RS1-RS2)*100.0/RS1
      PRINT 212,ZZZ
212   FORMAT(//50X,*PERCENT ERROR*,E12.5)
      PRINT 220,F,C,A,RS1,RS2,AB32
220   FORMAT(2X,E12.6,5X,E12.6,5X,E12.6,5X,E12.6,5X,E12.6,5X,E12.6)
      RRS1=1.0+F*(1.0+AB32/3.0)
      RRS1=F*(1.0+AB32)/RRS1
      RRS1=0.653*SQRT(RRS1)
      WWW=3.0+2.0*F+2.0*(1.0-F)*(C**1.666)
      YYY=2.0+2.0*F+(3.0-2.0*F)*(C**1.666)
      RRS2=YYY-WWW*(C**0.333)
      RRS2=(1.0-C**1.666)*F/RRS2
      RRS2=0.923*SQRT(RRS2)
      PRINT 225,RRS1,RRS2
225   FORMAT(//10X,*SIRKAR=*,E12.5,** GAL-OR =*,E12.5)
      C=C+0.05
      IF (C-0.6) 85,500,500
500   CONTINUE
      STOP
      END
```

APPENDIX E

SIMPLIFICATION OF DRAG EXPRESSION FOR A CLOUD OF ELONGATED RODS

The prolate spheroid resembles a long thin rod if the semimajor axis, a, is much greater than the semiminor axis, b, such that

$$C = \sqrt{(a^2-b^2)} \cong \tag{E.1}$$

This approximation leads to

$$\text{Cosh } \beta_a = \frac{a}{C} \cong 1.0 \tag{E.2}$$

$$\text{Sinh } \beta_a = \frac{b}{C} = \frac{b}{a} \cong \frac{b}{a} \tag{E.3}$$

The general expression for the drag on a prolate spheroidal particle placed in a cloud of identical particles is given by (2.68)

$$F_z^* = \frac{8 \pi \mu a U^*}{G^*} \tag{2.68}$$

where

$$G^* = \frac{\text{Cosh } \beta_b}{\text{Sinh}^2 \beta_b} \text{ Sinh } \beta_a + (1 + \text{Cosh}^2 \beta_a) [\text{Coth}^{-1} \text{ Cosh } \beta_a$$
$$- \text{Coth}^{-1} \text{ Cosh } \beta_b] - \text{Cosh } \beta_a \tag{2.64}$$

Using (E.2) and (E.3) equation (2.64) reduces to

$$G^* = \frac{\text{Cosh } \beta_b}{\text{Sinh}^2 \beta_b} [\frac{b}{a}] - 2 \text{ Coth}^{-1} \text{ Cosh } \beta_b + 2\ln [\frac{a}{b}] + 2 \ln 2 - 1.0 \tag{E.4}$$

and

$$\text{Cosh } \beta_b = 2 \text{ Cosh } \beta_f - 1.0 \tag{E.5}$$

$$\text{Sinh } \beta_b = 2 \text{ Sinh } \beta_f - [\tfrac{b}{a}] \tag{E.6}$$

where

$$\text{Sinh}^2\beta_f \text{ Cosh } \beta_f = \frac{[b/a]^2}{(1-\varepsilon)} \tag{E.7}$$

and

$$\text{Cosh } \beta_f = \sqrt{(1 + \text{Sinh}^2\beta_f)}$$

$$\cong (1 + \text{Sinh } \beta_f - \tfrac{b}{a}) \tag{E.8}$$

Thus the drug on a elongated rod placed in a cloud of identica particles reduces to

$$F_z^* = \frac{8 \pi \mu a U^*}{\dfrac{\text{Cosh } \beta_b}{\text{Sinh}^2\beta_b} [\tfrac{b}{a}] - 2 \text{ Coth}^{-1}\text{Cosh } \beta_b + 2\ln [\tfrac{a}{b}] + 2\ln 2 - 1.0} \tag{E.9}$$

For a elongated rod particle placed in an infinite medium the expression (E.9) reduces to

$$F_z^* = \frac{4 \pi \mu a U^*}{\ln [\tfrac{a}{b}] + \ln 2 - 0.5} \tag{E.10}$$

which is identical to that obtained by Happel and Brenner [18]